LABORATORI NAZIONALI DI FRASCATI
SIS – Pubblicazioni

LNF–00/021(P)
13 Settembre 2000

DAΦNE Machine Project

Contributions to the
7th European Particle Accelerator Conference (EPAC 2000)
Austria Center Vienna, 26 to 30 June 2000

CONTENTS

Invited Talk

Status Report on DAΦNE Performances

M. Zobov for the DAΦNE Team..... 1

Contributed - Oral

Beam Measurements for Luminosity Optimisation in DAΦNE

F. Sannibale, C. Biscari, M. Boscolo, A. Drago, A. Gallo, A. Ghigo, S. Guiducci,
F. Marcellini, G. Mazzitelli, C. Milardi, M. Preger, M. Serio, A. Stella,
C. Vaccarezza, G. Vignola, M. Zobov 6

Contributed - Posters

Design Status of a High Harmonic RF System for DAΦNE

A. Gallo, A. Alesini, R. Boni, S. Guiducci, F. Marcellini, M. Zobov
and M. Migliorati, M. Palumbo, Rome Univ. "La Sapienza..... 9

Data Handling at DAΦNE

G. Di Pirro, G. Mazzitelli, A. Stecchi..... 12

Optics Measurements in DAΦNE

C. Milardi, G. Benedetti, C. Biscari, S. Di Mitri, M. Boscolo, A. Drago
S. Guiducci, G. Mazzitelli, M. Preger, C. Vaccarezza, G. Vignola, M. Zobov 15

The Evolution and Status of the DAΦNE Control System

G. Di Pirro, G. Mazzitelli, A. Stecchi 18

Hom Damping in the DAΦNE Injection Kickers

A. Ghigo, D. Alesini, A. Gallo, F. Marcellini, M. Serio 21

STATUS REPORT ON DAΦNE PERFORMANCE

M. Zobov, for the DAΦNE Commissioning Team[1], LNF-INFN, Frascati, Italy

Abstract

Commissioning of the Φ-factory DAΦNE with two temporary interaction regions was successfully concluded in November 1998 proving the reliability of all machine systems. After the roll-in of the experimental detector KLOE, the commissioning resumed and the beam was stored in this configuration at the end of March 1999. The first physics events were already observed in mid April 1999. Since then, the collider shares its time between experimental shifts and machine physics runs. The main efforts have been dedicated to push up the luminosity by improving the single bunch collision luminosity and increasing the current in multibunch operations. We describe the results achieved so far, discuss the difficulties encountered on the way to high luminosity and the actions undertaken to improve collider performance.

1 INTRODUCTION

DAΦNE, the Frascati 1.02 GeV c.m. electron/positron Φ-factory [1], is now in operation at Frascati Laboratories of Italian National Institute of Nuclear Physics. The main DAΦNE design parameters are listed in Table 1, while the magnetic layout is shown in Fig. 1.

Table 1: DAΦNE Design Parameters

Energy [GeV]	0.51
Trajectory length [m]	97.69
RF frequency [MHz]	368.26
Harmonic number	120
Damping time, τ_E/τ_x [ms]	17.8/36.0
Bunch length [cm]	3
Emittance, $\varepsilon_x/\varepsilon_y$ [mm·mrad]	1/0.01
Beta function, β_x^*, β_y^* [m]	4.5/0.045
Particles/bunch [10^{10}]	8.9
Single bunch luminosity [$cm^{-2}\,s^{-1}$]	$4.4\,10^{30}$

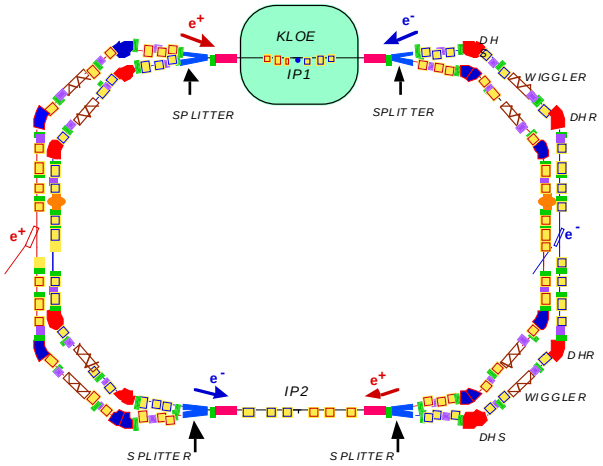

Figure 1: Main Rings magnetic layout.

High current, multibunch and flat beam approach has been adopted for DAΦNE, similar to that of PEP-II [2] and KEKB [3], to reach high luminosity. Electron and positron beams, stored in two separate rings, travel in a common vacuum chamber in the Interaction Regions (IR) and collide at two Interaction Points (IP). Crossing at a horizontal angle of 25 mrad minimizes the effect of parasitic collisions and allows to store many bunches, increasing the luminosity by a factor equal to the number of bunches. The DAΦNE design accepts a maximum number of 120 bunches and all the critical subsystems (injector, RF, vacuum system, diagnostics) are dimensioned to cope with a stored current of ~ 5 A.

The Phase I luminosity target is $10^{32}\ cm^{-2}\ s^{-1}$ with ~1A of average current stored in each colliding beam. Once this target is obtained, in parallel with physics runs, we will progressively tune the machine systems for higher currents and increase the number of bunches, and consequently the luminosity. In order to achieve this ultimate goal further investment on the longitudinal feedback and additional work on the cures of the parasitic crossings effects will be needed.

The DAΦNE commissioning with two provisional interaction regions without experimental detectors ("Day-one" IRs) was concluded successfully in November 1998 (see [4] for details). After the KLOE detector [5] installation the first beam was stored at the end of March 1999. Since then, the commissioning efforts have been dedicated to the compensation of the perturbation introduced in the machine optics by the experimental detector solenoid, to the optimization of beam parameters at the interaction point in order to improve the single

[1] D. Alesini, C. Biscari, G. Benedetti, R. Boni, M. Boscolo, A. Clozza, G. Delle Monache, S. Di Mitri, G. Di Pirro, A. Drago, A. Gallo, A. Ghigo, S. Guiducci, F. Marcellini, G. Mazzitelli, C. Milardi, L. Pellegrino, M.A. Preger, R. Ricci, C. Sanelli, F. Sannibale, M. Serio, F. Sgamma, A. Stecchi, A. Stella, C. Vaccarezza, M. Vescovi, G. Vignola, M. Zobov.

bunch collision luminosity and to increase the beam current in multibunch operation.

In this paper we give a brief description of the DAΦNE collider with the KLOE interaction region (IR), describe the results of the machine optics modelling and coupling correction, discuss beam dynamics in single and multibunch operation and analyse the data obtained in beam-beam collisions with the experimental detector.

2 GENERAL DESCRIPTION

The DAΦNE magnetic layout is shown in Fig. 1.

The circumference of each ring is about 100 m: this length is imposed by the need to have two 10 m long IRs. In each ring two sections connect the IRs: an outer one called Long and an inner one called Short. Each of these two sections is made of two arc cells with an utility straight section in between. The Short straight section is dispersion free and it is used for RF cavity, feedback kickers and diagnostics. The Long straight section is used for injection and diagnostics.

Particular care has been taken in the design to make the damping times as short as possible in order to counteract possible instabilities at the DAΦNE low energy. Small bending radius in the dipoles and four high field wigglers in each ring produce large energy loss. The energy radiated in the wigglers is about as much as that radiated in the bending magnets.

One of the parameters required to increase the luminosity is high emittance. The arc cell (BWB: bending-wiggler-bending) with two bendings and a wiggler in between them has been designed to increase the emitted radiation and tune the emittance. The cell is a double bend achromat with three quadrupoles (DFF) and a wiggler inside; a chromaticity correction sextupole is placed on each side of the wiggler. One of the dipoles has parallel end faces allowing better separation of the optical functions at the sextupoles. By varying the dispersion function in the wiggler the emittance can be tuned over a wide range.

3 KLOE IR

The KLOE detector consists of a cylindrical drift chamber surrounded by a lead-scintillating fiber electromagnetic calorimeter and immersed in the 0.6 T magnetic field of a 2.5 m radius superconducting solenoid. In order to leave the maximum free solid angle for the experiment the low-β triplets, which are embedded inside the detector on either side of the IP, are realized with permanent magnet quadrupoles. The three quadrupoles of each triplet are confined inside a cone of 9° half-aperture and the free space around the IP is ±0.45 m thus providing a solid angle of 99% available for the detector.

The integrated field of the KLOE solenoid is ~ 2.4 Tm: this is a strong perturbation to the machine optics at the DAΦNE energy which corresponds to a rigidity of $B\rho = 1.7$ Tm. The KLOE solenoid rotates the normal modes of oscillation in the transverse plane by an angle of 41.5°. This is the major contribution to the coupling between radial and vertical oscillations.

The correction of such a large coupling is obtained by two compensating solenoids plus rotated permanent magnet quadrupoles: the rotation introduced by the solenoidal field of KLOE is neutralized by the two superconducting compensating solenoids of equal but opposite integrated field and symmetrically placed on each side of the detector. The low-β quadrupoles inserted in the detector solenoid do not affect the coupling correction provided they are tilted by an angle equal to the rotation angle due to the solenoid.

4 LATTICE MODEL

DAΦNE optics modeling is not a simple task due to the high complexity of the magnetic layout including wigglers and experimental detector solenoids as an integral part, the absence of periodicity and the close vicinity of the two rings, leading to substantial crosstalk. The machine model is based on magnetic measurements of all the elements, measurements of the optical functions and Response Matrix (RM) analysis.

The present optical model takes into account:

- Splitter and dipole magnet fringing fields.
- Wiggler fringing fields and focusing on the trajectory due to the quadratic term in the vertical field.
- Longitudinal solenoid field distribution of KLOE detector and compensator solenoids.
- Longitudinal behavior of the gradient of the permanent magnet quadrupoles in KLOE low beta insertion, which, due to the small ratio between the gap and magnetic length, is not well represented by the step model.
- Tilt of these quadrupoles which compensate the transverse rotation introduced by the KLOE solenoid.

The model reproduces the beta functions within 5% accuracy, the tunes within 0.01 (0.2% of the absolute value), the dispersion function within few cm, the emittance within 10% and the momentum compaction within 1%.

The present optics model allows to correct the vertical dispersion down to 100 μm, thus removing this coupling source, gives a possibility to explore wide tune areas during luminosity tune up without changing the model parameters, to tune the emittance and momentum compaction, helps to adjust the optics functions at the sextupole positions in order to obtain more efficient chromaticity correction and to improve the dynamic aperture.

As the result of the modeling the DAΦNE optics has been optimized. Now the magnet currents of both rings are similar and the orbits, beta functions, dispersions and momentum compaction are almost equal in the two rings.

The small tune difference in the two rings of the order of 0.05 is due to the stray fields of the transfer line magnets, which introduce an asymmetry between the two ring lattices, and to the ion clearing electrodes in the electron ring.

5 COUPLING CORRECTION

The coupling correction is an important issue for DAΦNE since:

- Coupling must be reduced down to 1% in order to provide the design vertical beam size.
- Coupling may affect single ring transverse dynamics, in particular, the dynamic aperture.
- If not properly corrected, coupling may lead to luminosity degradation, inducing vertical size blow up and relative tilt angle between colliding bunches.

At the commissioning stage without solenoids it was demonstrated that the design tolerances on all the magnet alignments are well satisfied achieving coupling value of 0.4 %.

The coupling correction with the experimental solenoid is more complicated since it requires precise matching between low-beta quadrupole tilts, detector and compensator solenoids fields and the beam energy.

Survey measurements on the low-beta triplets done during the last winter shutdown showed a tilt misalignment of the order of 1^0, which therefore prevents the exact coupling correction.

Another source of coupling is in the second IR, where the beams are presently vertically separated and pass off-axis in the stray field of the splitter magnets. Fortunately, the phase of this perturbation is such that coupling can be controlled adjusting the KLOE IR parameters. Tuning the KLOE IR solenoid fields and the beam separation at the second IP can therefore optimize the coupling correction. In this way coupling has been corrected down to the values of 0.2% in the positron ring and 0.3% in the electron one without using any skew quadrupole.

The relevant improvement in the coupling correction was confirmed by beam size measurements at the synchrotron light monitor and observing correlated reduction in the beam lifetime that in DAΦNE is essentially dominated by the Touschek effect.

More information about coupling has been obtained from RM measurements. The average ratio between vertical and horizontal displacement caused by all horizontal steering magnets at each BPM is taken as a measurement of the average amount of horizontal oscillation transferred to the vertical plane, i.e. proportional to the tilt angle introduced by coupling sources along the machine.

Figure 2 compares this value before and after the coupling correction.

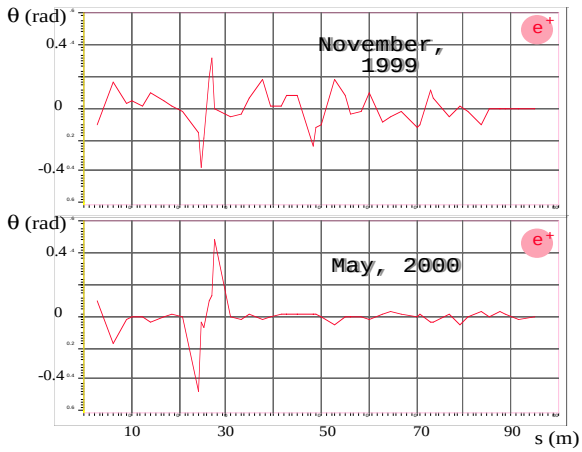

Figure 2: Transverse tilt measurements in the positron ring by response matrix analysis.

6 BEAM DYNAMICS

6.1 Single Beam Dynamics

Before the detector installation the maximum current stored in single bunch mode in both rings was 110 mA, i.e. by a factor of 2.5 higher than the design value of 44 mA. No destructive single bunch instability was observed.

The bunch length as a function of bunch current has been measured in the positron ring using a signal from the broad-band button pick up [6]. A very good agreement with numerical simulations based on machine impedance estimates has been found. According to these data the normalized coupling impedance |Z/n| is below 0.6 Ω. Recently, the measurements were repeated in both rings with a streak camera. The results agree well with those obtained with the button for the positron ring. In the electron ring bunches are measured to be about 20-30% longer than positron bunches since the electron ring impedance is higher, presumably due to the presence of several clearing electrodes.

After the experimental IR installation, an unstable quadrupole mode was detected in both rings. It has been found that the mode threshold is very sensitive to the bunch length. In particular, the threshold was higher for lower RF voltages and higher momentum compaction. Moreover, the instability disappeared by increasing the bunch current above a certain threshold. Perhaps, this can be explained by a modification of the impedance at high frequencies where the quadrupole mode spectrum has a maximum. An increase of the bunch length shifts the mode spectrum to lower frequencies and the current instability threshold increases.

The instability problem has been fixed by increasing the momentum compaction and by applying HOM damping antennas in the injection kickers [7].

At present, no sign of microwave instability is observed at different RF voltages up to a single bunch current of 140 mA. No dedicated measurements were carried out to estimate the exact value of the transverse impedance since some observations have shown that it is low. In particular, a head-tail instability threshold as high as 13 mA with sextupoles off has been achieved after an accurate orbit correction. Moreover, the observed vertical tune shift is a small fraction of the synchrotron tune in the whole current range from zero to the nominal value, indicating that the DAΦNE operating point is quite far from the transverse mode coupling threshold.

6.2 Multibunch operation

So far no major problems for multibunch operation in DAΦNE have been encountered. The maximum stored currents have exceeded 1 A in both the positron and the electron rings. Further current increase is limited by bad vacuum after a vacuum accident in April 2000 when cooling water from a synchrotron light copper absorber penetrated into the vacuum chamber. We expect to reach higher currents when vacuum is improved.

Figure 3 shows the DCCT record for the positron ring. The current of about 1050 mA was stored in 60 equidistant bunches. The beam was stable at that point even without a transverse feedback. However, sometimes we observe transverse dipole coherent oscillations in the positron beam at lower currents. The instability does not represent a serious danger for the beam since the coherent oscillations are damped in beam-beam collisions due to Landau damping.

Figure 3: DCCT current record in the positron ring.

In order to reach higher currents and to improve beam stability additional investments are being made in feedback systems. Recently, a new filter was implemented in the longitudinal feedback system, allowing to overcome the 0-mode instability. A prototype transverse feedback system has already been installed in the positron ring and has proven to perform well.

7 BEAM-BEAM INTERACTION

7.1 Collision point optimization

In order to achieve high luminosity the longitudinal and transverse positions of the two beams must be adjusted to provide maximum overlap at the IP. Moreover, the waists of the vertical beta functions of the two rings should coincide with the crossing point.

The longitudinal overlap of colliding bunches at the nominal IP has been synchronized by monitoring the distance between the combined signals of the two beams on two sets of symmetric BPMs on either side of the IP. The final precise longitudinal timing has been achieved by varying the RF phase of one of the two beams in order to maximize the luminosity monitor signal.

The beam orbit measurements in the IRs are performed by six BPMs distributed along each IR. Since the position of both beams is measured by the same monitors, monitor offsets cancel out. Averaging over 100 BPM readings provides precise beam position measurements in the IRs with a standard deviation below 10 μm. Closed orbit bumps in the IR with four correctors are applied to adjust angle and displacement at the IP and overlap the beams. Orbit bumps have been also used to separate vertically the beams in one of the IRs when colliding in only one IP.

At present the optimization of the beam collision parameters is performed by measuring the luminosity as a function of calibrated vertical and horizontal bumps at the IP. The fit of these dependencies gives us the mean geometric rms beam sizes ($\Sigma_{x,y}$) at the collision point which have to be minimized.

Figure 4 shows the luminosity as a function of the vertical bump at the IP measured by the luminosity monitor.

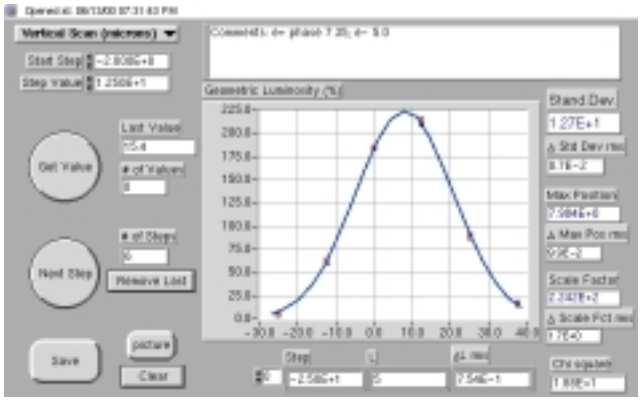

Figure 4: Σy measurement by luminosity scan.

By optimizing the coupling in the best case we have reduced the vertical capital sigma Σ_y down to 13 μm, while the nominal value is more that twice higher (30 μm).

7.2 Experimental results

After KLOE detector installation it was decided to exploit the same working point as we had used during "Day One" commissioning since quite satisfactory luminosity in single bunch collisions of 1.6E30 $cm^{-2}s^{-1}$ was obtained [8]. Working on that point in December 1999 allowed us to deliver to the KLOE experiment data taking runs with lifetime of 1 hour and initial luminosity of 4.5E30 $cm^{-2}s^{-1}$ with about 300-400 mA stored in 30-40 bunches and to collect an integrated luminosity of ~2.5 pb^{-1} during approximately 1 month of physics runs.

Further luminosity improvement was limited by the maximum achievable luminosity in single bunch collisions which at that time was at the level of 1-2E29 $cm^{-2}s^{-1}$.

One possible explanation of this limit is the imperfect correction of coupling. Indeed, as the numerical simulations show, beam blow up depends strongly on coupling and, in particular, on how and where in the ring it is created. In the collider configuration with the KLOE detector there are new sources of coupling such as rotation errors of the KLOE IR permanent quadrupoles. Furthermore, it has also been found that the coupling depends on the beam separation bump at the second IP.

Another possible reason could be stronger sextupolar nonlinearities in the lattice with the KLOE IR due to necessity to correct a higher natural chromaticity. Crosstalk between beam-beam effects and machine nonlinearities is one of the subjects presently under study.

After a collider shut down in January-February 2000 the main efforts are dedicated to improve the single bunch luminosity. By adjusting the collision point parameters and decreasing the coupling we have managed to increase the single bunch luminosity up to 5-6E29 $cm^{-2}s^{-1}$.

In multibunch operation the luminosity scales linearly with the number of bunches.

Figure 5 shows the luminosity measured by the detector for different number of bunches. The maximum luminosity of 1.0E31 $cm^{-2}s^{-1}$ has been achieved in 30 bunch configuration with about 350 mA per beam. Unfortunately, because of the recent vacuum accident we could not use more bunches to push the luminosity up since the residual gas pressure increases too much at higher currents.

Our present activity is aimed at improving the single bunch luminosity performance by exploring new tune areas, performing careful coupling correction and collision point optimization. In parallel, we use high current beam vacuum chamber conditioning in order to reduce the residual gas pressure allowing high current multibunch luminosity collisions.

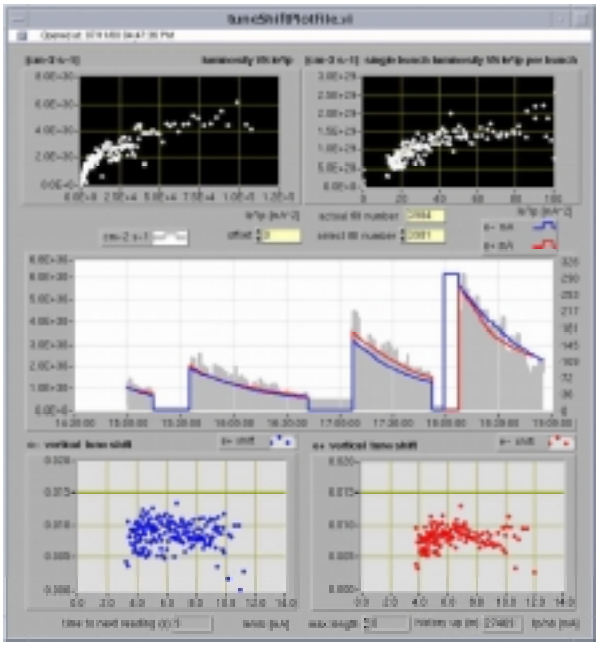

Figure 5: Luminosity measurement for 6, 10, 20 and 29 bunches per each beam, respectively (with 10 mA per bunch).

8 ACKNOWLEDGMENTS

The work described in this paper could not be realized without the commitment of all the technical staff of the LNF Accelerator Division. Pina Possanza is acknowledged for her patience and skill in editing the manuscript.

9 REFERENCES

[1] G. Vignola, and DAΦNE Project Team, DAΦNE, The Frascati Φ-factory, Proc. of PAC '93, Washington.

[2] J.T. Seeman, Commissioning Results of B-Factories, Proc. of PAC '99, New York.

[3] K. Oide, The KEKB Commissioning Team, Commissioning of the KEKB B-Factory, Proc. of PAC '99, New York.

[4] S. Guiducci for the DAΦNE Commissioning Team, DAΦNE Operating Experience, Proc. of PAC '99, New York.

[5] The KLOE Collaboration, KLOE a General Purpose Detector for DAΦNE, LNF-92/019(IR), April 1992.

[6] A. Gallo for the DAΦNE Commissioning Team, Single and Multibunch Beam Dynamics Study During the DAΦNE Main Ring Commissioning, KEK Proceedings 99-24, February 2000.

[7] A. Ghigo et. al., WEP5B06, this Conference.

[8] M. Zobov et. al., Beam-Beam Interactions in DAΦNE: Numerical Simulations and Experimental Results, KEK Proceedings 99-24, February 2000.

BEAM MEASUREMENTS FOR LUMINOSITY OPTIMISATION IN DAΦNE

F. Sannibale, C. Biscari, M. Boscolo, G. Di Pirro, A. Drago, A. Gallo, A. Ghigo, S. Guiducci, F. Marcellini, G. Mazzitelli, C. Milardi, M. Preger, M. Serio, A. Stecchi, A. Stella, C. Vaccarezza, G. Vignola, M. Zobov, INFN-LNF, Frascati, Italy

Abstract

The optimisation of the DAΦNE interaction region for luminosity performances passes through a number of beam measurements that allow to set the proper overlap of the colliding beams and to minimize the beam-beam effects that degrade luminosity. Most of the machine diagnostics systems are involved in this process and in particular a machine dedicated luminosity monitor, the tune measurement system, the synchrotron light monitor and the orbit acquisition system play a fundamental role. In the present paper a description of the most significant measurements is presented.

1 INTRODUCTION

Among the existing factories, DAΦNE [1] has the lowest energy (0.51 GeV/beam). The KLOE experiment detector, placed in one of the two interaction regions, makes use of a solenoid magnet whose integrated field is about 2.1 Tm. This combination of low energy beam and strong solenoidal field in the interaction region (IR) induces a large coupling that must be carefully compensated in order to improve the luminosity performance. In fact commissioning experience and beam-beam simulations [1], have indicated the existence of a very bad synergism between beam-beam effects and coupling. In particular, the presence of even modest values of coupling can significantly enhance the vertical beam blow-up with consequent luminosity reduction. For this reason the coupling, generated in the KLOE IR and in any other source along the machine, must be corrected as much as possible. At present time emittance ratios as low as 0.2% have been obtained (the design value is 1.0%).

At the same time the other parameters at the interaction point (IP) (optical functions, vertical crossing angle, vertical overlap, …) that, in a flat beam machine such as DAΦNE, play an important role in the beam-beam game must be tuned with a great accuracy.

The optimisation of these machine parameters needs accurate measurements. Because of the KLOE requirement of a large material free region around the IP, very little space was left for the IR diagnostics, which has a reduced configuration, particularly for what concerns the number of beam position monitors. The optimisation of the IP parameters passes through indirect measurements performed by basically all the DAΦNE diagnostic systems [2]. The synchrotron light monitor, the orbit acquisition system and the tune measurement system [3, 4, 5], play an important role, but the fine tuning of the beam-beam affecting parameters is obtained by a machine dedicated luminosity monitor [6]. This is a high counting rate monitor, able to perform fast measurements with small fluctuation, in 2 or 3 seconds, allowing a real time optimisation of the machine parameters.

This paper deals with the most significant beam measurements performed in the final tuning phase. Table 1 shows the DAΦNE parameters, while a complete update of the present performances can be found in [1].

Table 1: DAΦNE Design Parameters

Energy	0.51 GeV/beam
Phase 1 Luminosity (30 bunches)	1.3 10^{32} cm^{-2} s^{-1}
Final Luminosity (120 bunches)	5.2 10^{32} cm^{-2} s^{-1}
Beta Functions @ IP (V/H)	4.5/450 cm
Natural Emittance	10^{-6} m rad
Emittance Ratio	0.01
Particles/Bunch (Max)	8.9 10^{10}
Beam-beam Tune Shift (Max) (V/H)	0.04/0.04
Horizontal Crossing Angle	10-15 mrad
r.m.s. Bunch Length	3 10^{-2} m
Natural Relative Energy Spread	4 10^{-4}
Number of Bunches (Max)	120
Ring Length	97.69 m
RF Frequency	368.263 MHz

2 BEAM MEASUREMENTS IN NON BEAM-BEAM REGIME

The IR parameters are first optimised in a condition of negligible beam-beam effects. Such a situation is achieved when very small currents per bunch are stored in both rings (typically less than 1 mA/bunch). Multibunch mode is preferred in order to increase the counting rate at the luminosity monitor improving the measurement accuracy.

Most of the measurements make use of the luminosity parameter scan technique where a machine parameter is systematically varied and the effects on luminosity are recorded.

2.1 Overlap at IP of the Colliding Beams

Among the possible scans, the ones concerning the mutual beam position at IP are very useful. They allow to directly measure the quantities Σ_y and Σ_x:

$$\Sigma_w = \sqrt{\sigma_{w+}^2 + \sigma_{w-}^2} \qquad w = x, y \tag{1}$$

that appear in the luminosity formula:

$$L = f_R \frac{N^+ N^-}{2\pi \Sigma_x \Sigma_y} \tag{2}$$

Figure 1 shows an example of a vertical position scan. With the beams in collision, the electron beam vertical position at IP is changed with a 5 μm step and the related luminosity is measured. Data are fitted by a gaussian function that gives Σ_y, the best overlap position y_{max} and the luminosity maximum value. Luminosities are normalised to the product of the colliding currents and referred to the design value of 2.27 10^{27} cm^{-2} s^{-1} mA^{-2}.

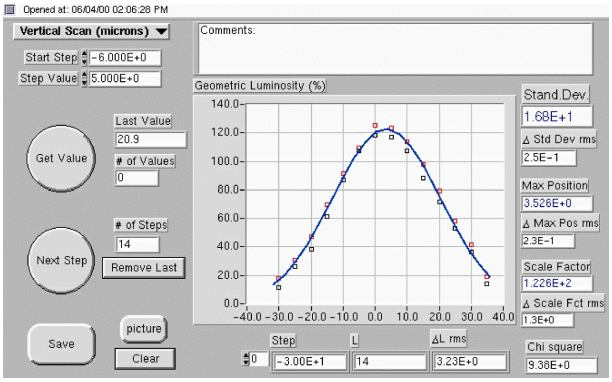

Figure 1: Luminosity vs. Vertical Position@IP.

Luminosity and the Σ parameters are measured and their consistency with the expected values calculated by equations (1) and (2) can be checked. Any discrepancy, taking into account the experimental errors, is an indication of a non-properly set IP: presence, for example, of relative transverse tilt between the colliding beams, vertical dispersion, different optical functions. In Figure 1, the measured Σ_y of 16.8 μm is, using the values of Table 1, a clear indication of a well-overlapped IP consistent with a coupling corrected down to 0.3 % in both beams.

2.2 Best IP Position and Vertical Crossing Angle Correction.

DAΦNE is a separate ring collider with independent e^+ and e^- RF cavities. By changing the RF phase of one of these cavities it is possible to move the longitudinal position of the IP. If vertical position scans are performed at different IP positions, then the dependence of Σ_y and of y_{max} with respect to the IP position can be measured. By using the first set of data and assuming zero vertical dispersion at IP and negligible effects due to bunch length, than equation (1) gives a quadratic dependence of the square of Σ_y with respect to the IP position s_{IP}:

$$\Sigma_y^2 = a_2 s_{IP}^2 + a_1 s_{IP} + a_0 \qquad (3)$$

By equation (3) it is possible to fit the data and find the IP position where Σ_y assumes its minimum value. In separated rings machines where the optical functions at the IR and in particular the vertical beta waist position, can be different in the two rings, this minimum Σ_y identifies the IP position that gives the best luminosity performance obtainable with that IR configuration.

Figure 2 shows an example of such a measurement.

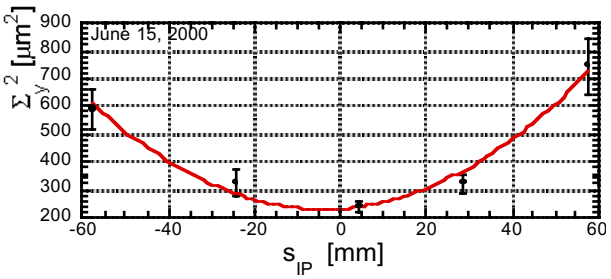

Figure 2: IP Best Longitudinal Position Measurement.

The detector solenoidal field introduces a coupling between the coordinates of the transverse plane. A rotation of the reference frame proportional to the field integral along the longitudinal direction decouples the transverse plane again. It can be shown that in this rotated reference frame (RRF) the difference between the vertical trajectories of the beam center of mass of the colliding beams is, with a very good approximation:

$$\Delta y_{c.m.} = \left(y'^{+}_{IP} - y'^{-}_{IP}\right) s_{IP} \qquad (4)$$

Any position scan, including the vertical, is performed in RRF, thus the best overlap position y_{max} is a measurement of $\Delta y_{c.m.}$. If y_{max} vs. the IP position s_{IP} is fitted by equation (4) then the slope of the fit is a measurement of the beam vertical crossing angle at IP.

Figure 3 shows a measured vertical crossing angle of ~ 230 μrad (dashed line) and a residual angle of less than 70 μrad (solid line) after the correction performed by a vertical angle bump localized at IP.

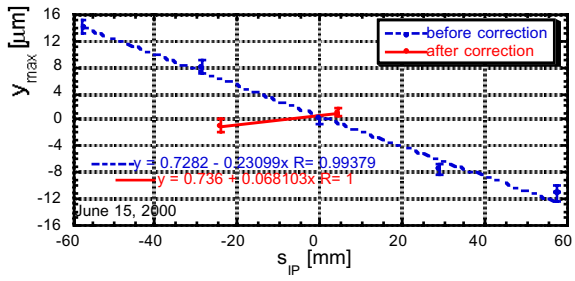

Figure 3. Vertical Crossing Angle Measurement

2.3 Vertical Dispersion and Transverse Plane Coupling at IP.

The y_{max} value, obtained by a vertical position scan, can also be used for estimating the vertical dispersion and the transverse plane coupling at IP.

In the first case a vertical scan is taken and the related y_{max} value is recorded. After that, the beam energy is changed by applying a RF shift Δf_{RF} and a new vertical scan is performed. The difference between the two values of y_{max} obtained at the different energies is a measurement

of the vertical dispersion at IP. Actually, because of the common RF source, such a measurement does not give the absolute value of the vertical dispersion but just the difference between the dispersions of the two beams at IP.

In the transverse coupling case, the measurement starts with two scans, one vertical and the other horizontal, in order to get the initial values of y_{max} and x_{max}. The second step consists in powering in one of the rings, outside the IR, a horizontal corrector. The corrector kick must be strong enough to generate a horizontal closed orbit distortion at IP of the same order of the horizontal beam size. New vertical and horizontal position scans are finally performed and the ratio between the differences of the new and old values of y_{max} and x_{max} gives a measure of transverse plane coupling at IP.

3 BEAM MEASUREMENTS IN BEAM-BEAM REGIME

When the current of the colliding bunches increases the beam-beam effects become more and more important up to limit the maximum achievable luminosity. An exhaustive beam-beam theory does not exist, simulations can address the choices, but the final tuning must be performed by beam measurements.

3.1 Beam-beam Tune Shift.

The knowledge of the beam-beam tune shift vs. the single beam colliding currents gives a clear picture of the beam-beam scenario. This quantity can be evaluated by measuring, in the tune monitor, the associated coherent tune shift. The ratio between the coherent and incoherent tune shifts is a function that depends on a number of parameters [7] and its evaluation is often tricky. Additionally, at present time, the DAΦNE rings have different working points. This situation not only changes the mentioned ratio [8] but, reducing the beam-beam induced coherent oscillation, also makes the measurements difficult. An alternative way to obtain the tune shifts is given by the expressions:

$$\xi_y^{\pm} = \frac{2r_e}{\gamma f_R}\beta_y^* \frac{L}{N^{\pm}} \qquad \xi_x^{\pm} = \frac{r_e}{2\pi\gamma}\frac{N^{\mp}}{\varepsilon} \tag{5}$$

that hold for flat and equal beams. In DAΦNE the vertical tune shift is evaluated at each luminosity measurement, allowing, for example, a run time measurements of the maximum tune shift achievable with that machine configuration.

3.2 Beam-beam Blow-up.

In a flat beam collider the beam-beam induced vertical blow-up is the ultimate limit to luminosity. The intensity of this effect depends on several parameters as, tune resonances, lattice non-linearities and all the coupling components. In collision, these quantities can be tuned by moving the proper knob (working point for tunes resonances, sextupoles strength for non-linearities, skew quadrupoles strength for coupling) and maximizing the luminosity or, equivalently, minimizing the beam-beam vertical blow-up. In DAΦNE it is possible to put the beams in and out of collision, in a very clean way, by applying or removing a RF phase jump of 2, 3 or 4 π in one of the cavities. The roundness values *R* (ratio between the vertical and horizontal beam dimensions at the synchrotron light monitor) in and out of collision are recorded at each knob variation step. The ratio R_{in}/R_{out} is a measure of the blow-up and its minimum indicates the best setting for that knob. Figure 4 shows an example of such a measurement where the current of a positron skew is varied and the related luminosities (dashed line) and positron roundness ratios (solid line) are recorded.

Additional information on single beam non-linearities minimization in DAΦNE can be found in [9].

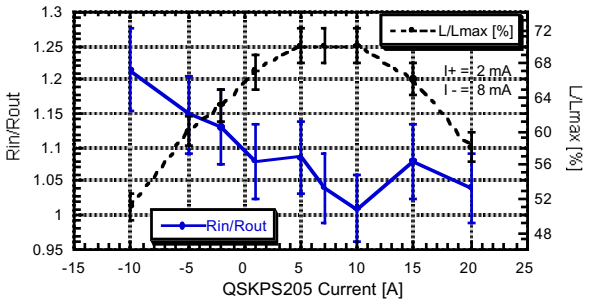

Figure 4: Positron Skew Quadrupole Scan.

AKNOWLEDGEMENTS

The authors want to express their appreciation to P. Raimondi for his pyrotechnic contribution in control room, during the last two weeks of June.

REFERENCES

[1] M. Zobov, "Status Report on DAΦNE Performance", this Conference.

[2] F. Sannibale et al., "Luminosity Optimisation in DAΦNE ", DIPAC99, Chester, UK, 16-18 May 1999.

[3] A. Ghigo, F. Sannibale, M. Serio, "Synchrotron Radiation Monitor for DAΦNE", BIW 94, Vancouver, Oct. 1994.

[4] A. Stella et al., "Beam Position Monitor System of DAΦNE", BIW 98, Stanford, May 1998.

[5] A. Ghigo et al., "DAΦNE Beam Instrumentation", BIW 98, Stanford, May 1998.

[6] G. Di Pirro et al., "The DAΦNE Luminosity Monitor", BIW 98, Stanford, May 1998.

[7] K. Yokoya et al., "Tune Shift of Coherent Beam-Beam Oscillations", KEK Preprint 89-14, May 1989 A.

[8] A. Hofmann, "Beam-Beam Modes for Two Beams with Unequal Tunes", LHC99 Beam-Beam Workshop.

[9] C. Milardi et al., "Optics Measurements in DAΦNE", this Conference.

DESIGN STATUS OF A HIGH HARMONIC RF SYSTEM FOR DAΦNE

A. Gallo, D. Alesini, R. Boni, S. Guiducci, F. Marcellini, M. Zobov, INFN-LNF Frascati;
M. Migliorati, L. Palumbo, Rome Univ. "La Sapienza" and INFN-LNF Frascati

Abstract

The Φ-Factory DAΦNE, a 1 GeV c.m. high luminosity double ring collider, is presently in operation at the Frascati Laboratories of INFN. The study and the design of a high harmonic RF system, aimed to increase the bunch length and to add Landau damping through the broadening of the synchrotron tune spread, is in progress. The bunch lengthening will provide better beam lifetime (which is Touschek dominated at the DA ΦNE energy) and will decrease the interaction between the beam and the high-frequency part of the machine impedance. A larger Landau damping is also expected to contribute to the stabilization of the beam dynamics. In this paper we report the beam dynamics study in the presence of the harmonic RF system, with special attention to the impact on the performances of the bunch-by-bunch longitudinal feedback system. Comparison between the passive and active mode of operation is also presented.

1 INTRODUCTION

The need for a harmonic RF system in the DAΦNE main rings has become evident during the luminosity tune-up of the machine [1]. To increase the single bunch luminosity the coupling factor in both rings has been decreased, thus reducing the beam lifetime.

The best values of single bunch luminosity have been obtained typically with 10÷15 mA per bunch, with a bunch length of 2÷2.5 cm and a RF voltage of 120 kV. Since the nominal bunch length value is 3 cm, we have a margin to increase both the bunch length and the acceptance by rising the main RF voltage and adding a harmonic voltage with an opposite slope on the bunch. In this case the bunch length can be kept always at about its nominal value, with the maximum energy acceptance available. An improvement of the Touschek lifetime is expected, and the gain factors for different scenarios have been calculated and are reported in this paper.

The bunch lengthening and the Landau damping due to the increased synchrotron tune spread are also expected to give a beneficial contribution to the machine dynamics, in particular concerning the microwave regime [2, 3].

On the other hand, the harmonic voltage significantly perturbs the longitudinal beam dynamics, the most concerning issues being the shift of the coupled-bunch mode "0", "1" and "N-1" coherent frequencies (N is the number of regularly spaced bunches) and the synchronous phase spread along a bunch train with a gap.The expected performance of the high harmonic system is discussed and a comparison of the various options is given in the paper.

2 DESIGN PARAMETERS

The aim of the harmonic system is to keep the rms bunch length at $\sigma_z \approx 3$ cm. Since the short-range wakefields always contributes to the bunch lengthening, the harmonic system has been designed to work with a natural bunch length of $\sigma_{z0} \approx 2$cm. The harmonic voltage necessary to get the required bunch length is obtained by solving the Haissinski equation. In Table 1 the voltages required to have $\sigma_{z0} \approx 2$ cm for RF harmonic number 2, 3 and 4 are shown, together with the expected synchrotron frequency values and their variation for oscillations of 1 σ_{z0} amplitude. The RF voltage is V_{RF}= 200 kV, the momentum compaction is α_c = 0.02, and the harmonic voltage is assumed to be 90° out of phase with respect to the harmonic of the beam current, in order to have only pure reactive beam loading on the harmonic RF system.

Table 1: Basic Parameters

n of RF harmonic	2	3	4
f_{RF_H} [MHz]	736.53	1104.8	1473.1
V_{RF_H} [kV]	81	57	45
f_S [kHz]	15.15	13.42	10.6
$\Delta f_S(@\sigma_{z0})$ [kHz]	0.54	1.63	3.55

The harmonic voltages reported in Table 1 do not scale exactly as 1/n, and the synchrotron frequency (i.e. the slope of the overall RF voltage) is not constant for different harmonic choices. This is due to the non-linearity of the harmonic voltage over the bunch length.

The required harmonic voltage can be obtained by powering a cavity with an external RF source (active option) or by letting the beam current interact with the harmonic cavity fundamental mode impedance (passive option). In the latter case the cavity has to be progressively detuned upward as the current increases in order to keep the harmonic voltage constant.

The passive option is more attractive since it is much simpler and cheaper. On the other hand, the active option is already effective at zero current, and allows single bunch measurements in lengthening regime.

3 COHERENT FREQUENCY SHIFT

The shift of the coherent synchrotron frequencies of the coupled bunch (CB) dipole modes is given by [4]:

$$j(\omega_c - \omega_s) \approx \frac{I_b \alpha_c \; p\omega_0^2 \exp\left(-p^2\omega_0^2\sigma_t^2\right)}{4\pi \; \omega_s \; E/e} Z_L\left(p\omega_0 + \omega_s\right) \quad (1)$$

where $p = kN + M$, M designates the CB mode, ω_0 is the revolution angular frequency, ω_c and ω_s are the coherent

and incoherent synchrotron angular frequencies, σ_t is the bunch rms duration, E/e is the beam energy , and Z_L is the longitudinal coupling impedance. This formula, which is accurate only for small shifts, indicates that the imaginary part of Z_L changes the frequency of the CB coherent oscillations. Too large shifts are not tolerable for the bunch-by-bunch longitudinal feedback system [5] (LFB) which damps coherent oscillations in a limited band around the unperturbed synchrotron frequency.

In an active RF harmonic system the cavity is always tuned nearby $n\omega_{RF}$, and the imaginary part of the fundamental mode impedance interacts only with the CB mode "0" (the beam barycentric motion). In this case the interaction between the beam and the fundamental mode impedance can be reduced by means of active feedback techniques including the RF power source [6].

In the case of a passive harmonic cavity the situation is quite different since the fundamental mode impedance, depending on the beam current, is tuned in between $n\omega_{RF}$ and $n\omega_{RF}+\omega_0$, and its imaginary part interacts also with the CB modes "1" and "N-1". An existing time-domain tracking code [7] has been adapted to study the CB dynamics in presence of a passive harmonic cavity. The code tracks the motion of macroparticles in the longitudinal phase space in the presence of longitudinal resonant modes and includes radiation damping and realistic models for the RF and the LFB systems.

4 SIMULATIONS OF UNIFORM BEAMS

To study the CB dynamics related to the shift of the coherent synchrotron frequencies, the motion of uniformly filled beam has been simulated in the time domain. The frequency of the coherent CB modes is obtained by FFT transforming the output of the tracking code.

The frequency of the coherent CB modes as a function of the beam current is shown in Fig. 1 in the case of .a passive 4th harmonic cavity.

Modes different from "0","1" and "N-1" do not show significant frequency shift since there are no resonant impedances interacting with them in the simulations. The CB mode "0" interacts with both main and harmonic cavity impedances and its coherent frequency , according to the simulations, is largely shifted up. The agreement with eq. 1 is not very good, since in this case the shift is a result of two very large contributions of opposite signs, while eq. 1 is valid only for small frequency shifts. Anyway, although the LFB system is not effective on it, the "0" mode motion is stabilized by Robinson damping.

The CB modes "1" and "N-1" interact with the harmonic cavity and their coherent frequency decreases. In this case, which is less peculiar with respect to that of mode "0", the agreement with eq. 1 is much better. The frequency decreases only by ≈ 35% for a beam current increase from 0 to 1.2 A, and the LFB system can be tuned in such a way that it will be effective for all CB modes (except the mode"0") in that current range.

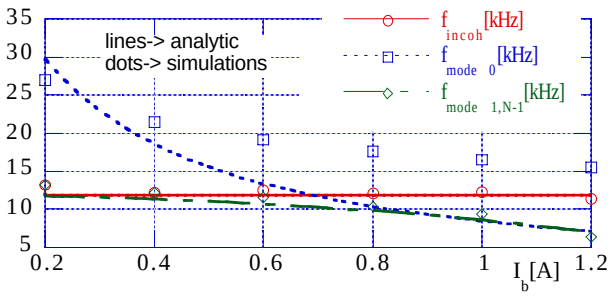

Figure 1: Shift of the CB mode coherent frequencies.

The harmonic cavity R/Q value plays a crucial role in the previous results. The larger it is, the more the cavity has to be detuned to keep the voltage constant, and the larger is the frequency shift of the modes "1" and "N-1". A large R/Q, which is desirable for an active cavity, may be very unsuitable for a passive cavity.

According to both simulations and eq. 1, the coherent frequency shift of CB modes 1" and "N-1" is less critic for lower harmonic numbers (n=2,3).

5 SIMULATIONS OF BEAMS WITH GAP

The operational configuration of the DAΦNE beam consists in a bunch train with ≈30% gap to avoid ion trapping in the e^- ring.

The presence of the gap substantially complicates the analytical approach of the CB motion, since the concept of CB spatial mode has to be deeply revised. We follow a numerical approach in this case, which consists in running the time-domain tracking code and interpreting the output results by means of physical arguments.

It is well known that different bunches in a train with a gap are subject to different long-range wakefields, resulting in different values of the energy loss per turn or, in other words, in a parasitic loss spread along the train. If the train interacts mainly with imaginary impedance, the average of this spread is zero.

The parasitic loss spread is converted in a synchronous phase spread along the train, since every bunch is positioned at the RF phase corresponding to its energy loss per turn. The primary effect of the harmonic cavity on that is to produce a large magnification of the synchronous phase spread since the local slope of the total RF voltage at the bunch position is lowered by the harmonic component. The parasitic loss spread is also increased by the contribution of the harmonic cavity impedance to the long-range wakefields. Because of the harmonic voltage non-linearity, each bunch acquires its own synchrotron frequency, shape, length and lifetime.

The bunch train distribution over the total RF voltage, the synchrotron frequency and the natural length of the bunches along the train and the charge distribution in the first, central and last bunches are shown in Fig. 2, in the case of a 3rd harmonic cavity for a current of 1.2 A in a 40 bunch train filling 2/3 of the ring.

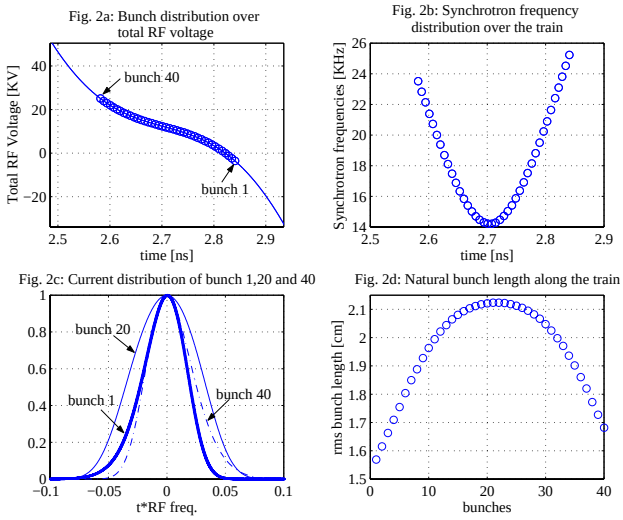

Figure 2: Effects of the gap on the bunch characteristics.

The spread of the synchrotron frequencies produces a decoherence in the CB motion acting as a sort of bunch-by-bunch Landau damping. We observe this effect in the simulations. In fact, the simulated CB dynamics looks more critical in the 2nd harmonic case, where the total RF voltage is linear on a wider phase range.

Anyway, large values of synchronous phase spread may change the interaction point (IP) position leading to luminosity degradation. They affect also the synchronism of the LFB front-end and back-end, limiting the system performances. We believe that these effects set the ultimate operational limits to the RF harmonic system. From this point of view the active and passive options are equivalent, with the annotation that low R/Q cavities give smaller contributions to the synchronous phase spread.

6 BUNCH LENGTHENING AND LIFETIME

The short range wakefields tends to reduce the differences in length and Touschek lifetime from bunch to bunch in trains with a gap. In order to study the single bunch dynamics including the higher harmonic cavity, we have adapted a single bunch tracking code already used to estimate the DAΦNE bunch length [3].

The results of the simulations are shown in Fig. 3. The solid line represents the bunch length as a function of the bunch number for a 3rd harmonic cavity with a current of 1.2 A in a 40 bunch train with a gap of 1/3rd of the ring. The σ_z values vary from 2.4 cm of the last bunch, which has an almost triangular shape (see Fig. 4) to 2.8 cm of the central one, having a more symmetrical shape.

The longitudinal charge distribution $\rho(z)$ given by the code and the RF acceptance of each bunch have been considered to calculate its own Touschek lifetime [8].

In Fig. 3 the dotted line represents the expected gain in Touschek lifetime with respect to a routinely DAΦNE operating configuration, where the RF voltage is typically set to 120 kV.

The calculated improvement is in the 35÷60% range depending on the bunch position over the train, and is due mainly to the bunch lengthening since the limited physical aperture of the acceptance increase vacuum chamber reduces the gain due to the RF.

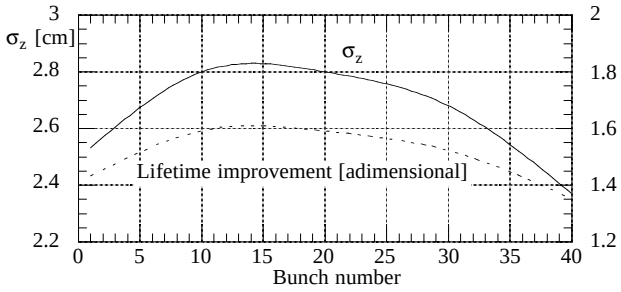

Figure 3: σ_z and lifetime gain for different bunches.

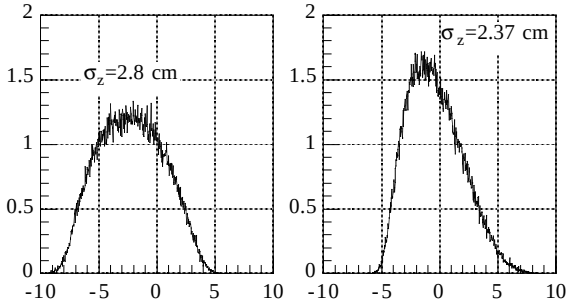

Figure 4: shapes of two different bunches (right: last bunch, left: central bunch).

CONCLUSIONS

The most important issue related to the implementation of a high harmonic RF system is the large synchronous phase spread of the bunches along intense trains with a gap. From this point of view active cavities, with high R/Q, are worse with respect to passive ones.

The coherent frequency shift of the CB modes “1” and “N-1” is relevant, but not destructive, in the passive option and it is less critic for low harmonic number (n=2,3), while it is not an issue in the active option.

Simulations of the CB dynamics of bunch trains filling 2/3 of the ring show that a 1.2 A is still stable when considering passive 3rd and 4th harmonic cavities.

We believe that a passive 3rd harmonic cavity is a simple and effective option.

REFERENCES

[1] M. Zobov et al., MOXE02, this conference.
[2] M. Migliorati et al., NIM A 354, 1995, p. 215.
[3] A. Gallo et al., KEK proc. 99-24, p.105.
[4] J.L. Laclare, CAS proc. CERN 87-03, Vol. I, p. 264.
[5] M. Serio et al, proc. of EPAC ’96, p. 148.
[6] D. Boussard, CAS proc. CERN 92-03, p. 474.
[7] M. Bassetti et al., DAΦNE tech. note G-19, 1993.
[8] A. Wrülich, CERN 94-01, Vol. I, p. 427.

DATA HANDLING TOOLS AT DAΦNE

G. Di Pirro, G. Mazzitelli, A. Stecchi, INFN-LNF, Frascati, Italy

Abstract

The DAΦNE collider has started operation with experiments since March 1999. A large amount of data is acquired. Several tools for data handling, storage, and presentation to machine operators and users have been developed and are available for online and offline analysis under most common information sharing systems such as WWW, cellular SMS and mailing. The general structure of the system, some examples of online information and users tools are presented.

1 INTRODUCTION

Data in the DAΦNE Control System [1] are stored in the local memories of the 42 front-end VME-CPUs distributed all over the accelerator area. The front-end tasks get commands from the high-level user environment and continually update their own data base with the information from the devices under control. Routines in the user environment are able to get data by a direct memory access to the front-end CPU's memory. The information in the front-end database is structured with different data types tailored to specific machine elements; this means that in order to get data or to correlate different devices specific routines must be implemented.

To be able to create a database for offline and online analysis and to correlate data of different devices, two system tasks have been developed. The offline database is accessible by users, experiments personnel, and operators through a World Wide Web server that takes care also of data consistency and provides information to authorized users via e-mail or via GSM SMS (Short Message Service) cellular phone.

2 SYSTEM TASKS

2.1 "Dumper"

Data distributed in the front-end memory are continuously fetched by a system task, called "Dumper". The procedure contains the specific data type of any device under control in the DAΦNE accelerator and writes data in a uniform database accessible from the high level user interface or other system tasks (see Fig. 1).

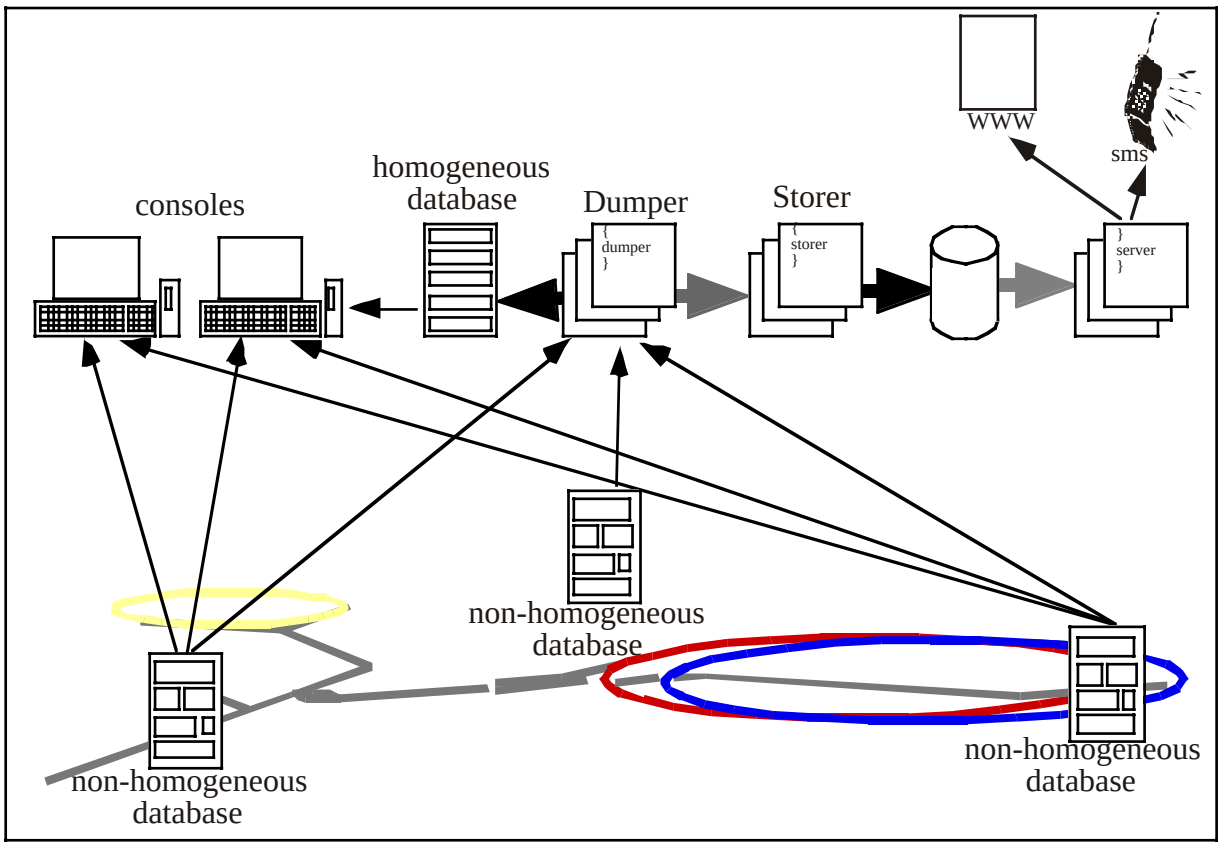

Figure 1: Schematic Layout of the System Tasks.

Some high-level user routines allow correlating a large amount of data. For example the "Hunter Dog" program continuously checks for faulty magnets, vacuum and low level CPUs.

Another program, "The Check Magnet Current Drift", allows to check the current oscillation and drift during operation.

2.2 "Storer"

The storage process of data for offline and slow online analysis is based on the Dumper uniform database. The task reads data from the dumper database, and stores on local disk a subset of the DAΦNE description. The disk is mirrored to an other authorized computer in the laboratory area. No handling is done on data at this level. This allows having full control on data for offline analysis, but requires some routines in order to extract meaningful information

2.3 The Storer Files System

The Storer files system is composed of two status files, with an update time of 5 seconds and 15 seconds each. The first one is used to provide information to satellite machines not belonging to the DAΦNE Control System environment, such as the longitudinal feedback[2], spectrum analyzer and so on. The second one is provided to experiments and is archived in a daily history for offline analysis. Data contain beam current, luminosity, machine status, bunch filling pattern, and some other accessory information.

A daily history file, recorded every 5 minutes, is also produced for elements with slow readout such as vacuum, magnet faults, etc. In this file the same information as in the fast status are also logged each minute file for easy data correlation. The mass storage is exported to machine for their own analysis and to the DAΦNE supervisor and WWW server for data presentation and pre-analysis.

3 DAΦNE SERVER

2.1 Online data handling

Data are stored without any handling. In order to provide users and experiments with useful information a task running on the DAΦNE server processes raw data and writes a new status and daily history file. According to the timing status, currents and luminosity a global machine status is obtained: **standby**, **injection e-**, **injection e+**, **stored e-**, **stored e+**, **filled**, **colliding**. Whenever the machine **filled** condition is reached a progressive number is incremented.

An important parameter for users is the beam lifetime estimation. A simple adaptive routine is applied on the current data when any of the **stored, filled** or **colliding** general condition is reached. As soon as the current data decays by a quantity greater than 10 times the noise of the current measurements, the lifetime is evaluated under linear approximation. This allows having a fast and quite accurate estimation of the beam lifetime.

The DAΦNE server takes care to produce files containing a subset of useful information easily accessible under control system or via Web. Figure 2 shows an example of correlation plot between KLOE luminosity and DAΦNE currents data. Some important parameters (luminosity per bunch, beam-beam tune shift) are estimated on line.

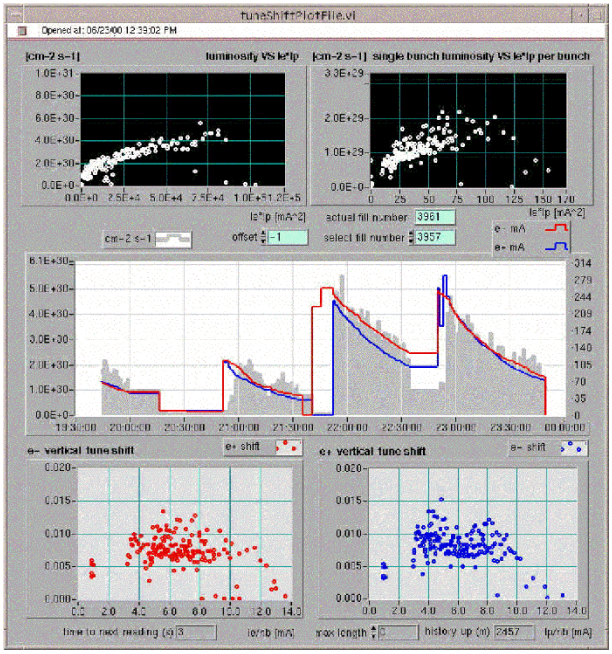

Figure 2: example of data correlation tools based on KLOE experiment data, and machine data.

2.2 The web and e-mail server

The DAΦNE server has been equipped with a Web server powered by Apache software. A set of CGIs (Common Gateway Interface) allows users to access online the DAΦNE and KLOE data. Statistics on run performance and daily information have been very useful in machine optimization.

Dedicated software written in the LabVIEW® environment has been developed for plots and histograms presentation.

A banner refreshed every 10 seconds continuously reports the status of the DAΦNE accelerator and of the main experiment KLOE (see Fig. 3).

A download area has been set for offline analysis, where not only stored data are accessible, but also machine settings and useful operating file can be obtained.

For safety the server is accessible only from the Laboratory domain on the other hand, a subset of most significant information are reported each minute in the Laboratory Web server.

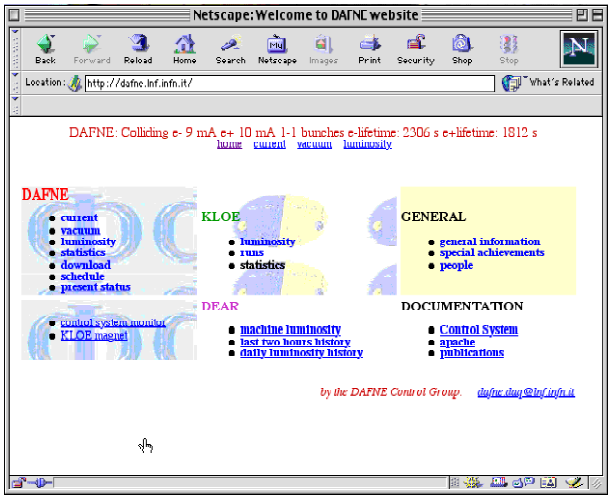

Figure 3: Welcome page of DAΦNE Website.

Authorized users can also download via e-mail most of the information available on the Web pages. The same routines elaborating data with CGIs return plain text information that can be received on demand or at scheduled time. A subset of information can be also sent via GSM SMS. A simple SMS query message can be sent by users to receive information on the DAΦNE-KLOE status. Midnight broadcast messages give a synthesis of the today's run performance.

2.3 Supervisor tools

A set of procedures running on the server continuously monitors the status of data acquisition and of the Control System. On line statistics of front-end tasks is available. Supervisor routines keep checking the data validity, and the health of the system task procedure. When some fault occurs in the Control System or in data acquisition system, specialized personnel are alerted via e-mail and GSM SMS.

4 CONCLUSION

A powerful system for DAΦNE machine data and KLOE experiment data as been implemented. During last year of operation the data handling tools have demonstrated useful for online data exchange, offline data analysis and machine optimization.

5 AKNOWLEDGMENT

We are very thanks to F. Murtas, P. Valente, who are working with us on the sharing of information with KLOE experiment and G. Baldini and M. Masciarelli who provided part of this job.

We also have to thank G. Vignola and F. Sannibale that coordinated and participated in the development of the data handling tools.

REFERENCES

[1] G. Di Pirro, G. Mazzitelli, A. Stecchi, “The Evolution and Status of the DAΦNE Control System”, TUP1B06 this Conference.

[2] J. Fox et al., "Programmable DSP-Based multi-bunch feedback - operational experience from six installations" BIW2000, Cambridge, Massachusetts.

OPTICS MEASUREMENTS IN DAΦNE

C. Milardi, G. Benedetti, C. Biscari, S. Di Mitri, M. Boscolo, A. Drago, S. Guiducci, G. Mazzitelli, M. Preger, C. Vaccarezza, G. Vignola, M. Zobov, INFN-LNF, Frascati, Italy

Abstract

In the two rings of the DAΦNE collider the presence of two Interaction Regions and of the experimental solenoid and the absence of periodicity make the assessment of the linear optics a challenging issue. Due to the low integer part of the tune, matching of the interaction parameters, emittance tuning or movements in the tune diagram always involve the whole ring optics: the collider model is therefore a critical tool to control luminosity. The Response Matrix is extensively used in the operation for closed orbit correction, localized bumps and especially in restoring the optimum luminosity conditions on the reference orbit. The Response Matrix information is also exploited for coupling analysis. Measurements on transverse space dynamic tracking are finally reported.

1 INTRODUCTION

DAΦNE [1] is a low energy, double ring, electron-positron collider. The two rings are symmetric and share two Interaction Regions (IRs). In one of them the KLOE [2] detector has been installed and is presently running.

The DAΦNE optics have been designed to optimize the single bunch luminosity. A reasonably large horizontal emittance, ε_x, limits the beam-beam tune shift for a given bunch charge. Four wigglers per ring placed in a dispersive region, inside the arcs, allow ε_x tunability. They introduce an extra radiation damping, welcome in a low energy ring in which the natural damping time corresponds to hundred thousand turns. Transverse coupling may excite resonances and seriously limit the single bunch luminosity by vertical emittance blowup, and colliding overlap reduction. The Kloe detector, with its 2.4 Tm solenoidal field, represents a strong perturbation to the collider lattice and may introduce a huge source of coupling if not properly compensated.

Luminosity is the last step of a collider tuning-up process. Accurate measurements of orbit, betatron functions, coupling, and dynamic aperture prelude to any luminosity achievement.

2 ORBIT

A fast orbit measurement system [3] is used extensively for position, dispersion and Response Matrix (RM) measurements. A *golden orbit* corresponds to the optimum luminosity set-up; restoring the *golden orbit* the best luminosity condition is immediately reproduced.

Closed orbit correction, beside the absolute orbit reduction, is aimed to the minimization of the transverse displacement in sextupoles, of the vertical dispersion and related coupling. It is performed using the orbit decomposition by eigenvalue of the measured RM, allowing to free the correction process from any model approximation and to minimize the corrector strengths. This method has been also used to compute localized displacement bumps. IP bumps, with the accuracy of the order of few μm, are routinely used for beam-beam scans and luminosity optimization [4].

3 MODEL

In the DAΦNE lattice the behaviour of the phase advance along the ring is tightly conditioned by the two IRs, the arcs, housing the wigglers, and the injection region. Flexibility is guaranteed by individually powered quadrupoles. Since any change in emittance, momentum compaction and tune involve the whole ring optics, a very reliable model is required. The first optical model of the rings was based on magnetic measurements of all the elements. Then measurements of betatron functions, dispersion and RM have been used to update the optical description of all the magnets. The betatron functions are measured by the gradient kick method in all quadrupoles. This method cannot be applied to the KLOE IR and its low beta quadrupoles, which are permanent magnet ones and have no steering coils. A variation in the compensator solenoid field is used to check the symmetry of the betatron functions around the IP and the position of the low-beta waists in the two rings.

The optical model takes into account:

- Splitter and dipole fringing fields.
- Wiggler fringing fields and focusing on the trajectory due to the quadratic term in the vertical field.
- Longitudinal behaviour of solenoid field of KLOE and C_2 and C_1 compensators.
- Longitudinal behaviour of the gradient of the permanent magnet quadrupoles in KLOE low beta, which due to the small ratio between gap and magnetic length are not well represented by the step model.
- Tilt of these quadrupoles, which compensate the transverse rotation introduced by the KLOE solenoid.

The two rings have the same magnetic structure. The difference between their tunes, with equal quadrupole settings, is of the order of $5*10^{-2}$, which correspond to 1% of the total tune. This difference is essentially due to the stray fields of the transfer line magnets, which introduce an asymmetry between the two ring lattices, and to the presence of ion clearing electrodes in the electron ring.

The model reproduces the betatron functions within 5% (see Fig. 1), the betatron tunes within 0.01 (0.2% of the

absolute value), the dispersion function within few cm (see Fig. 2), the emittance within 10% and the momentum compaction within 1%. All these features allow exploring different working points, as well as emittance and momentum compaction tuning.

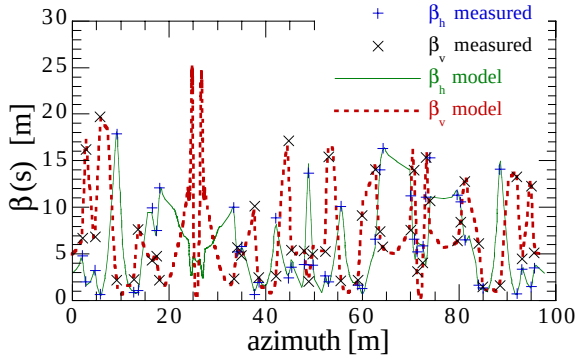

Figure1: Comparison between computed and measured betatron function for the electron ring.

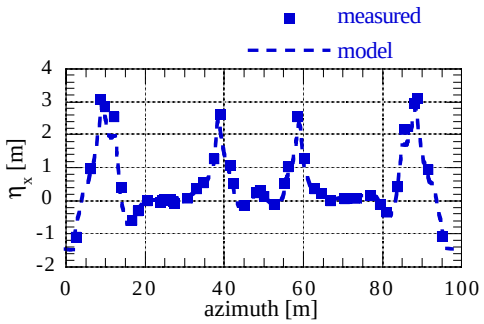

Figure 2: Comparison between computed and measured horizontal dispersion for the electron ring.

4 COUPLING

In DAΦNE the design beam-beam tune shifts in the horizontal and vertical plane are equal, obtained with 1% ratio between vertical and horizontal emittances and between vertical and horizontal β* (β at the IP). Just after the installation of the KLOE detector, tuning compensators and skew quadrupoles, the κ design value of 1% was obtained [5], but still the beam-beam behaviour was affected by coupling.

In the presence of coupling the betatron motion is no more purely horizontal and vertical [6]. Nevertheless it is still a combination of two independent modes, the pseudo-horizontal mode *a* and the pseudo-vertical mode *b*. The beam parameters at the IP are described in the normal mode formalism and the beam sizes depend on both modes. In a flat beam ring with no vertical dipoles, the emittance of the *b* mode, ε_b and therefore the coupling parameter κ, rise from transfer of amplitude oscillation of *a* mode around the ring. The contribution of any linear coupling source to ε_b is quadratic, while the contribution to the tilt of the pseudo-horizontal mode is linear. At the IP the decrease of luminosity due to coupling may come from large ε_b, relative tilt between the axis of the *a* modes in the two rings and from the projection of the *a* mode onto the vertical plane. The simulation analysis of the different coupling source in DAΦNE [7] [8] has shown that values of κ of the order of 1% are compatible with tilt values, at the IP, of the order of ±0.5%. Moreover the *a* mode projection in the vertical plane can even double the beam vertical size at the IP, depending on the source type and to its phase advance with respect to the IP. The κ design value of the order of 1% is therefore large for DAΦNE.

4.3 Coupling Correction

The design tolerances on all the magnet alignments in both rings are well satisfied, as demonstrated by the collider commissioning without Kloe, when values of κ of 0.4 % were obtained. The situation with the detector is well different, since the solenoidal compensation scheme cancel the coupling only if the low-beta quadrupole tilts and the beam rotation, introduced by detector and compensator fields, are exactly matched and the beam energy has its nominal value.

Survey measurements on the low-beta triplets, done in last winter shutdown, showed a tilt misalignment of the order of 1°, which therefore reduce the efficiency of the compensation method. Operative experience pointed out another source of coupling in the second IR, where beams are presently vertically separated and pass off–axis in the stray field of the adjacent splitter magnets. Simulation showed how this coupling source propagates around the ring with almost the same phase advance of a coupling source rising in the Kloe region. Tuning the solenoid fields and the beam separation in IP2 can therefore produce a global decoupling. Using this method the DAΦNE coupling has been corrected to values of 0.2% in the positron ring and 0.3% in the electron one, without using any skew quadrupole.

The more obvious measurement of the coupling is done at the Synchrotron Light Monitor. Beam-beam scans done at very low current [4], so not affected by beam-beam effect, provide a more accurate measurement of the dimension of the colliding beam overlap. Values of convoluted vertical sigma a factor 3 below the design ones confirm the SLM estimation.

Figure 3 presents the κ measurements as a function of the KLOE and compensator solenoidal field, square points correspond to the actual working configuration.

More information about the coupling has been obtained from the measured RM. The horizontal and vertical closed orbit distortion caused by all horizontal steerings, at each beam position monitor, are used to evaluate the average amount of horizontal oscillation transferred to the vertical plane. The transferred oscillation amplitude is presented as the slope, α, of the linear interpolation of the horizontal and vertical displacements at each azimuth along the machine. A comparison between ring configuration corresponding to different solenoid setups and κ values are presented in Fig. 4.

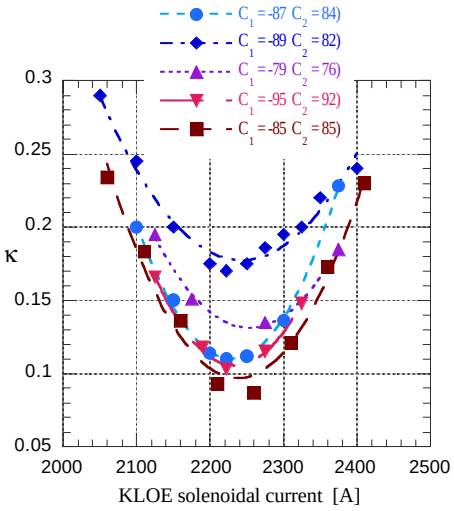

Figure 3: Measured κ value as a function of the KLOE and compensator solenoidal fields.

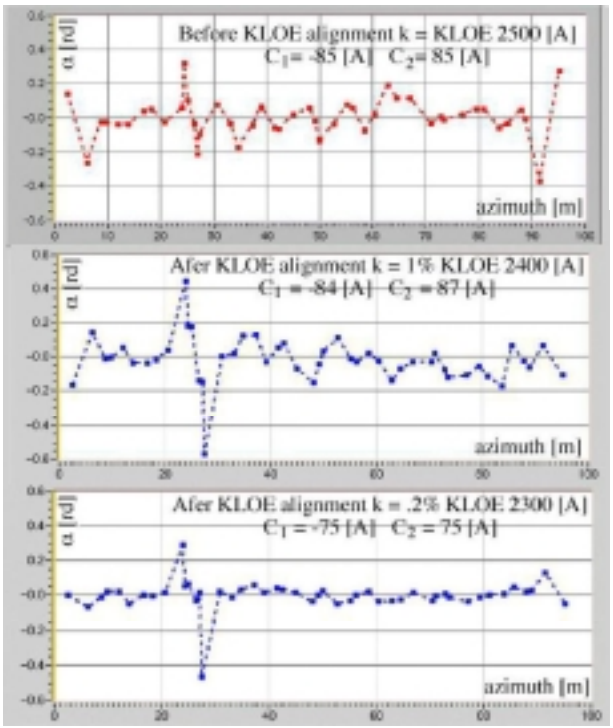

Figure 4: Average amount of horizontal oscillation transferred to the vertical plane as obtained from the measured RM.

5 TRANSVERSE SPACE ANALYSIS

The effect of machine non-linearity on the particle motion are investigated using a phase space monitor, a system allowing to store and analyze turn-by-turn the position of a kicked beam. A single bunch is excited horizontally pulsing one of the injection kickers. The coherent betatron oscillation amplitude is recorded over 2048 turns providing information on trajectories in the phase space and betatron tune shifts with amplitude. The coherent oscillation amplitude decay through nonlinear filamentation helps to estimate directly nonlinear tune spread due to the nonlinearities, and provides a quick tool to improve the dynamic aperture by varying sextupole settings.

Figure 5 shows an example of measured coherent oscillation decay and respective phase space trajectories, found by applying the Hilbert transform to the measured signal [9]. The seven branches in the phase space suggest that the betatron tune is close to the seventh order resonance.

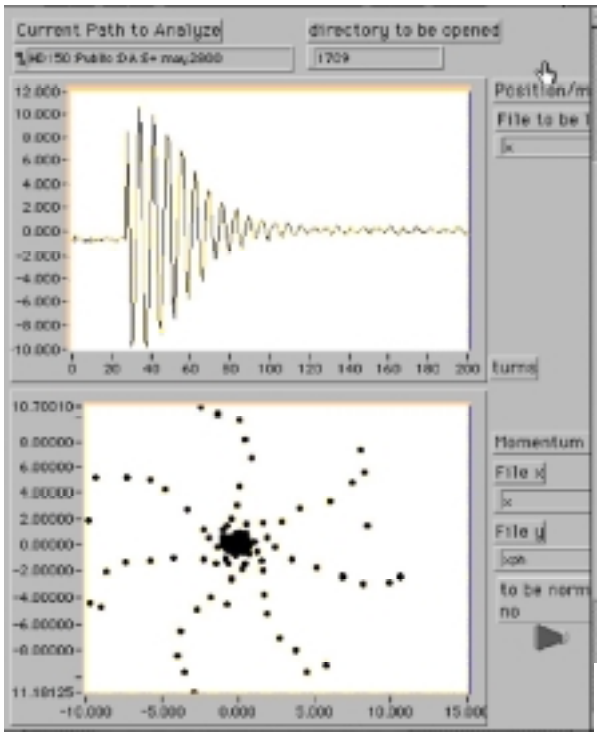

Figure 5: Coherent oscillation decay and corresponding phase space trajectories.

REFERENCES

[1] G. Vignola and DAΦNE Project Team "DAΦNE the Frascati Φ-factory", Proc. of PAC 93, Washington.

[2] The KLOE Collaboration "KLOE a General Purpose Detector for DAΦNE", LNF-92/019(IR), 1992.

[3] C. Milardi et al. "Integration of Diagnostics in the DAΦNE Control System", Proc. of DIPAC97, Frascati (RM), Italy, October 12-14, 1997.

[4] F. Sannibale et al., "Beam Measurements for Luminosity Optimization in DAΦNE", these Proceedings.

[5] C. Milardi for the DAΦNE Commissioning Team "Status of DAΦNE", DAΦNE 99, Frascati, Italy..

[6] P.P. Bagley, D.L. Rubin "Correction of transverse Coupling in a Storage Ring", EPAC'96, Sitges, June 1996.

[7] C. Biscari et al. "Coupling in DA_NE", DAΦNE Technical Note, L-30, March 3, 2000.

[8] C. Biscari "More about Coupling in DAΦNE", DAΦNE Technical Note, L-31, March 14, 2000.

[9] R.T. Burgess "The Hilbert Transform in tracking, mapping and multiturn beam measurements", CERN SL-Note-99-048 AP, 22 October 1999.

THE EVOLUTION AND STATUS OF THE DAΦNE CONTROL SYSTEM

G. Di Pirro, G. Mazzitelli, C. Milardi, F. Sannibale, A. Stecchi, A. Stella, INFN-LNF, Frascati

Abstract

During the DAΦNE commissioning and run operations the Control System has been continuously evolving in order to fulfill the user requirements and the needs of a complete accelerator management. The original structure of distributed CPUs relaying on a central shared memory proved to be scalable and suitable for adding functionality "on the fly". Also the choice of a commercial software environment for all the control tasks demonstrated to be valid and allowed redesigning the user level with no worries for porting all the developed software. Console applications have been moved from personal computers to Force® VME embedded processors and user interfaces now runs on a Sun® multiprocessor server connected to many lightweight SunRay® terminals. A comprehensive Control System evolution history is reported.

1 DESIGN STATEMENTS

Which is the major worry for people facing the design of an accelerator Control System?

No doubt: it is that the system works.

But what does it mean "to work"? Excluding disasters such as wrong topologies, poor bandwidth or CPU power, bugs in Operating Systems and so on, we can affirm that a Control System works when it allows to drive easily and reliably the accelerator.

The matter is how to gain this target: most likely there is not a golden way but certainly there is a coherent approach based on well-defined choices. When we started the DAΦNE [1] Control System [2] design, we decided to deal with commercial technologies as much as possible and this was for good reasons. A commercial object is characterized by a broad distribution, which means a lot of feedback from the users and consequently deep debugging. Furthermore the wider is the distribution of a product the more reliable is its support from the producer.

Another criterion was to privilege "easy development and maintenance".

We decided to use:

- personal computers with standard Operating Systems everywhere;
- LabVIEW[3] as development environment for all the software;
- industrial VME bus for front-end interfacement.

2 SYSTEM GENERAL DESCRIPTION

We distributed VME crates all around the machine in order to have the front-end hardware close to the devices to be controlled. We adopted as VME processors customized Macintosh® LCIII able to run LabVIEW code.

The distributed CPUs make up the system 3rd level where the applications dedicated to the device handling and control reside. All the CPUs run asynchronously and write into their own VME memory the result of the control tasks for all the devices of which they are in charge. The refresh time depends on the number of connected devices, on the complexity of the preprocessing implemented on the CPU and on the type of front-end connections. The CPU load (in terms of number of devices) is tuned in order to keep the control refresh rate within the desired value. Depending on the needs, this rate ranges from few Hz to 50 Hz even though dedicated applications could allow significantly higher rates.

From a data point of view the system 3rd level consists of several local memory pages where all the machine objects are represented as descriptive records continuously updated at their own rate. All 3rd level VME crates are connected to a central cluster of VMEs through point-to-point optical links to constitute a central common addressing space called 2nd level.

The 2nd level can be logically thought as a single bus thanks to a *crate interconnect* VMV [4] system.

The end result is a central virtual memory where the machine RTDB (Real Time Database) resides. Once the system has been properly initialized, the transaction from the 2nd up to the 3rd level is transparent to the user that can fetch any descriptive record from a remote memory page with a simple VME read cycle. These read actions are performed from the system 1st level, where the consoles and the user applications reside.

3 SYSTEM 1 IMPLEMENTATION

For the first system version we used Macintoshes 68040 as consoles.

The connection between the 1st and the 2nd level was done by plugging into each Macintosh NuBus a dedicated VMV interface and connecting in multidrop all the consoles up to the first 2nd level VME through a VMV branch.

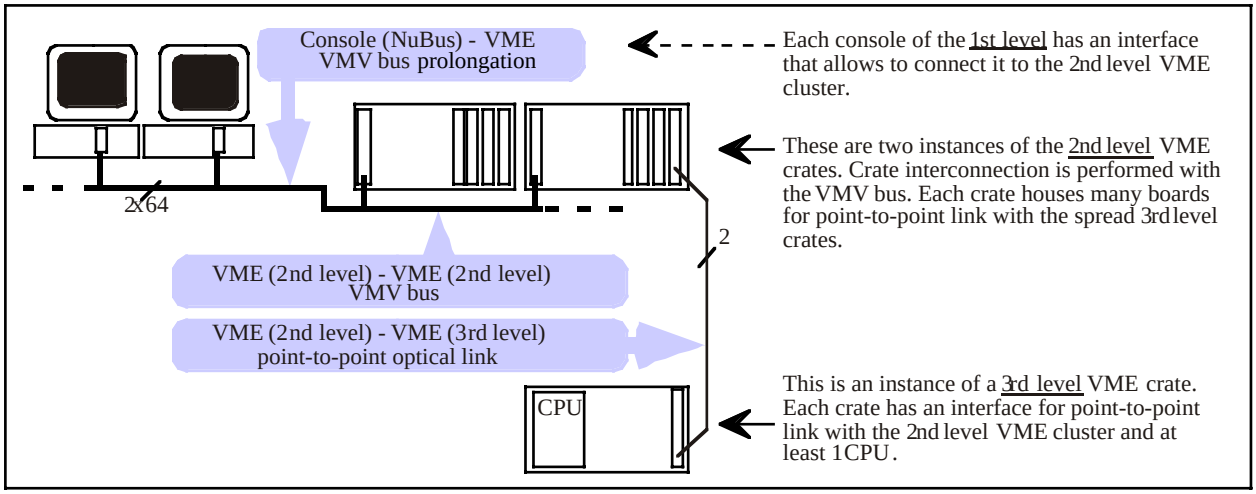

Figure 1: First implementation of the DAΦNE Control System. The consoles at 1st level were personal computers (Macintosh 68040) capable to access the central shared memory through dedicated internal interfaces.

The system version 1 (Fig. 1) main peculiarities were:

- "true" memory mapping of the central virtual memory into the consoles internal address space;
- uniform hardware and OS (Macintosh at any level);
- full accomplishment of the " Design statements".

The DAΦNE commissioning started and continued until December 1999 with this setup. The overall system behavior was good enough even though since the beginning we had to deal with a large number of bus errors due to two distinct causes.

First: the Macintosh NuBus timeout for a read/write cycle is 20.5 μs and when two or more consoles attempted to fetch simultaneously data from the shared memory, some of them could run in timeout.

Second: the Macintosh interfaces dedicated to VMV bus connection demonstrated to be not reliable in a such populated setup (we had 7 consoles and 7 VME crates on a single VMV branch) both for the arbitration and the bus current load. The workaround was to introduce software arbitration at the 2nd level and to split the VMV bus into two branches: one for the consoles and one for the 2nd level VMEs.

After this tune-up the system became more stable and grew smoothly following the introduction of new devices and the requests coming from the commissioning staff.

4 SYSTEM UPGRADE

Why to upgrade something which is working? In our case the general answer was that after 5 years of operation the system had reached some intrinsic limits:

- the Macintosh NuBus platform was dismissed;
- the 68040 μP was no longer able to stand the load of always-heavier requirements;
- the VMV consoles branch limited the number of installable consoles to about 10.

Moreover, the affirmation of new services based on Internet and the trend of "big" computers to be much easier and smarter pointed out that the choice of stand alone personal computers was no longer the most straightforward.

We focussed on the following upgrade targets:

- improve the overall system reliability;
- remove the consoles connection bus and therefore the limit to the number of consoles;
- enhance the consoles performances;
- gain remote access on the consoles;
- have Internet media and services fully available.

5 SYSTEM 2 IMPLEMENTATION

The system general structure based on distributed CPUs and a central shared memory demonstrated to be valid with no limitations from the hardware. It allowed easy and fast data gathering and correlation with no bandwidth worries.

Also the distributed processors showed to be suitable for the front-end tasks hence we focussed on the 1st level for the upgrade project. An obvious issue was to reuse as much as possible the software already developed and this somehow imposed to adopt computers able to run LabVIEW. Fortunately during last years LabVIEW had a spectacular affirmation in the industrial automation field as well as in the scientific community so that it was available on almost all the major platforms.

We adopted Spark 50T[5] VME embedded computers by FORCE instead of the Macintosh consoles. The 50T runs Solaris and is 100% compatible with the Sun UltraSpark Iii architecture. The first benefit of using VME embedded processors was to get rid of all bus-to-bus interfaces and cables and to gain RTDB data access without software arbitration.

First of all we developed the VME read/write basic routines and then we encapsulated them into conventional LabVIEW graphic nodes. After this, the porting of all the user applications in LabVIEW for Solaris went on smoothly and required just a little cosmetic make-up and a few minor adjustments.

The Spark 50 T is a multi-user machine and we estimated to load up to 5 sessions on each of them.

We installed four diskless 50T and a Sun Enterprise 250 as server over an Ethernet 100 Mbps switched network. The access to the user applications, which run on the VME processors, is done by mean of *SunRay*[6] lightweight terminals. These terminals are centrally managed by, and draw their computing resources from the *SunRay* server software that runs on the Enterprise 250.

The system performance, concerning the graphic presentations and the window management, greatly improved and also console hangs due to low memory disappeared. This architecture (Fig. 2) is fully scalable: it is possible to increase the number of VME embedded processors and hence the CPU power dedicated to user applications and to add "on the fly" *SunRay* terminals in order to have more working points.

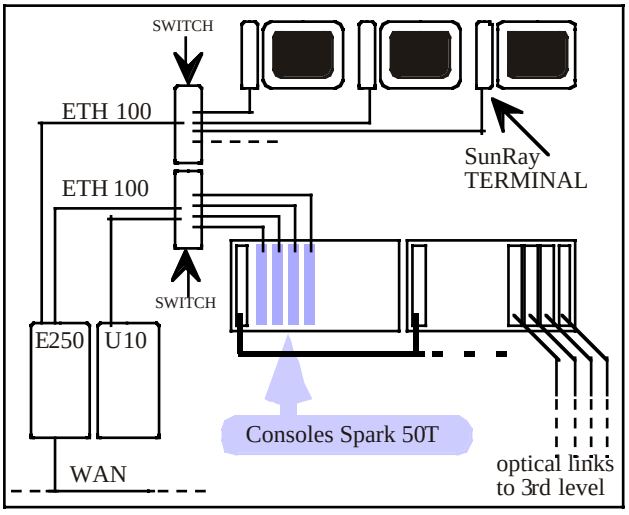

Figure 2: Second implementation of the Control System. The VME consoles and the SunRay terminals are on two separate ETH 100 Mbps switched networks.

Now the Control System integrates acquisition, disk storage and WWW online publishing [7] of machine data as well as dynamic data interchange with the experiment computing center.

CONCLUSIONS

After 6 months of development, tests and debugging and 3 months for the installation, the new system meets all the upgrade targets and is driving the accelerator since March 2000 (Table 1 summarizes the number and type of processors employed in the system in its present status).

Table 1: System main components

3rd level CPUs	Custom Mac LCIII MC68030	43
2nd level CPUs	FORCE 50T UltraSpark II	4
1nd level term.	SunRay MicroSpark	15
system server	Sun Enterprise 250 2 x UltraSPARC II	1
WWW server	Sun Ultra 10 UltraSpark II	1

ACKNOWLEDGEMENTS

We want to thank G. Baldini and M. Masciarelli for their commitment and essential contribution in the system implementation, O. Coiro and D. Pellegrini for their support in the hardware installation and setup, I. Sfiligoi for its contribution in the UNIX configuration and management.

We are also grateful to all the Accelerator Division staff for their continuous suggestions and stimulus for making a good and useful job.

REFERENCES

[1] G. Vignola and DAΦNE Project Team, DAΦNE: The First Φ-Factory, EPAC'96, Sitges, June 1996, p. 22.

[2] G. Di Pirro et al. "DANTE: Control System for DAΦNE based on Macintosh and LabView", Nuclear Instrument an Methods in Physics Research A 352 (1994) 455-475.

[3] LabVIEW, National Instruments Corporation, 11500 N Mopac Expwy, Austin, TX 78759-3504 USA (http://www.ni.com).

[4] Creative Electronic System S.A., Route du Pont-Butin 70 CH-1213 Petit-Lancy 1 Geneva Switzerland (http://www.ces.ch).

[5] Force Computers GmbH, Prof.-Messerschmitt-Str. 1, D-85579 Neubiberg/München., (http://www.forcecomputers.com).

[6] Sun Microsystems, Inc., 901 San Antonio Road, Palo Alto, CA 94303 USA (http://www.sun.com).

[7] G. Di Pirro, G. Mazzitelli, A. Stecchi, “Data handling tools at DAΦNE”, TUP1B04 this Conference.

HOM DAMPING IN THE DAΦNE INJECTION KICKERS

A. Ghigo, D. Alesini, A. Gallo, F. Marcellini, M. Serio, M. Zobov, INFN-LNF Frascati

Abstract

The maximum current per beam colliding in the Frascati Φ-Factory DAΦNE was limited by vertical multibunch instability. Investigations with the beam and measurements on the injection kicker prototypes evidenced several high order modes (HOM) trapped in the injection kickers structure, responsible for the instability. The dangerous HOM can be extracted by inserting a couple of wide bandwidth antennas in the kicker structure. The bench measurements on the modified kickers installed in the machine are reported.

1 INTRODUCTION

The operation of the Frascati Φ-Factory DAΦNE needs very high electron and positron currents stored in up to 120 bunches. During the commissioning longitudinal and transverse multibunch instabilities have been observed. The powerful longitudinal bunch by bunch feedback systems [1] are able to damp the longitudinal oscillation at the currents achieved so far (1 A for each beam). A vertical oscillation has been repeatedly observed and damped by keeping the chromaticity strongly positive (at the expence of lifetime shortening). Modal analysis and measurements of the instability threshold as a function of local orbit distortion put in evidence the beam interaction with some parasitic resonant mode trapped in the injection kicker regions. The structure has been studied with a theoretical model and computer simulations based on HFSS code [2]. Measurements on the prototype convinced us that two small antennas placed close to the coils return connections are able to damp the mode impedance to a negligible value without distortion of the kicker pulsed field.

2 INJECTION KICKER

2.1 Kicker Structure

Three fast kickers in each DAΦNE Main Ring allow single turn/single bunch injection. Each kicker is realized with four rods inside the vacuum chamber that has the same inner diameter of the rest of the straight section in order to avoid tapers and relative trapped HOM. The rods distance is compatible with the necessary stay-clear aperture. The two inner and outer rods are connected in series by two copper strips facing the vacuum chamber, as shown in Fig.1, forming two coils. The upper and lower coils are parallel connected to the vacuum feedthrough to halve the inductance presented to the power pulser [3].

The connection between the kicker inner structure, the external high voltage pulser and ground is accomplished by means of two feedthroughs with low profile ceramic insulators.

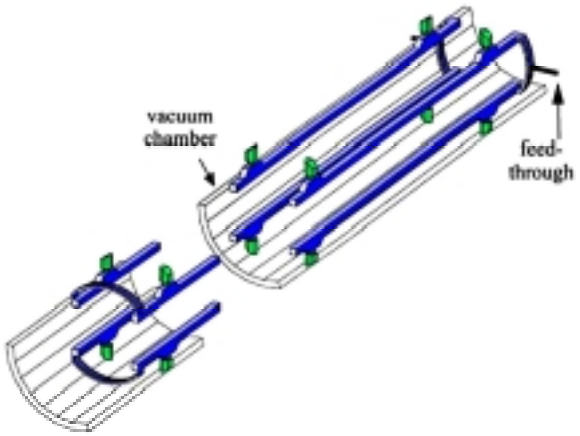

Figure 1: The injection kicker structure

A thyratron switch pulser discharges a capacitor into the kicker coils inductance. The current flowing in the kicker coils generates the pulsed magnetic field necessary to kick the bunch horizontally.

2.2 Kicker Model

A transmission line model has been adopted to study the frequency of the resonant trapped modes in the kicker. The field intensity and distribution have been determined also by computer simulation. The kicker has been considered as a multiconductor transmission line terminated on a reactive load that models the discontinuity between the coils and the vacuum chamber. By choosing a set of independent modes with the same symmetry of the kicker in the transverse plane, the study of the resonances of the complete multiconductor structure is reduced to the study of the resonances of four simple uncoupled transmission lines. The modal analysis is helpful in understanding which trapped mode interacts with the beam. In such a model no feedthrough and external connections are considered; therefore the damping due to the connections with the external device (pulser, ground connection) are not evaluated. The only loads of the multiconductor transmission line are simulated with capacitors permitting the calculation of the resonant frequencies and the distribution of voltage and current along the structure for each mode.

2.3 *Computer Simulations*

The kicker structure has been simulated with 3D-computer electromagnetic code HFSS with proper boundary conditions in order to calculate:

- the configuration of the transverse electric and magnetic fields along the structure;
- the distribution of the longitudinal component of the electric field along the structure, used for the calculation of the coupling impedance;
- the behavior of the electric or magnetic field at any section of the structure.

Figure 2 shows the portion of structure used in the HFSS simulation with the damping antenna and the exciting probe.

The frequencies and shunt resistances for the same resonances calculated with the analytical model and by computer simulations are shown in Table I.

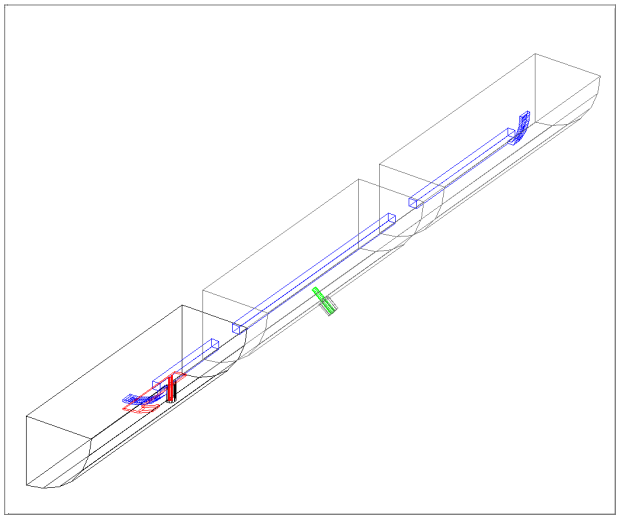

Figure 2: Kicker structure used in the HFSS simulations.

The longitudinal modes have two maxima of electric field at the end of the rods, therefore they are partially coupled and extracted by the connection between the rods and the external devices.

The horizontal modes have a maximum of electric field located at the feedthroughs side and a zero on the other side, then they are strongly damped. Viceversa, in the vertical case the maximum of electric field is in the opposite side where there are no external connection then the modes are completely trapped.

Table I: Results obtained with the transmission line model (t.l.m.) and HFSS simulation.

	freq. (t.l.m.) [MHz]	freq. (HFSS) [MHz]	Q_0 (HFSS)	R_s [Ω]
Longitudinal modes	861.31	838.4	2520	1171
	1005.60	979.3	3124	1459
	1440.14	1406.5	3386	1099
	1731.22	1690.6	3803	1040
	2169.73	2111.3	4611	1173
	freq. (t.l.m.) [MHz]	**freq. (HFSS) [MHz]**	**Q_0 (HFSS)**	**R_s [KΩ/m]**
Transverse modes	73.73	70.9	750	8080.0
	221.21	212.8	1670	1782.7
	368.69	355.1	1693	801.34

2.3 *HOM damping*

A damping antenna has been introduced to extract the dangerous modes trapped in the structure (see Fig. 3). It is realized by means of a strip electrically coupled with the resonant field and positioned under the connecting strips of the rods.

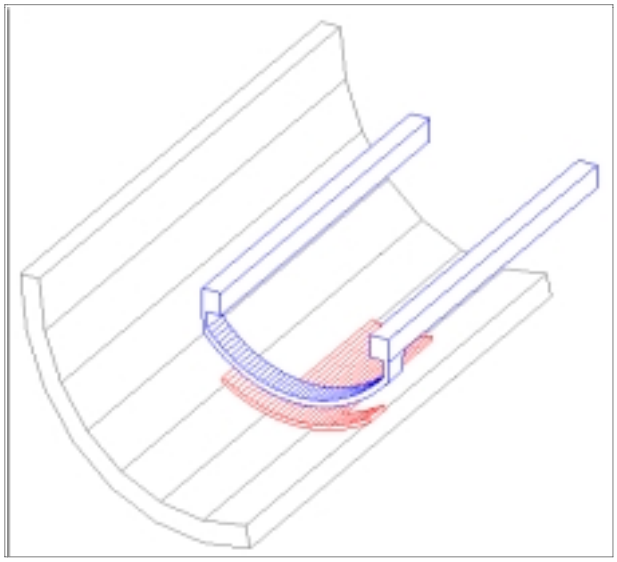

Figure 3: Kicker section in the damping antenna region.

The antenna is made of a copper plate with the same dimension and curvature of the connection strip. The antenna is connected to a 50Ω coaxial cable via a matched strip line connection. The connection strip is necessary to place the 50Ω vacuum feedthrough in a mechanically accessible point.

The antenna is a typical high pass filter because of the capacitive coupling with the field in the structure. In particular, reducing the distance between the antenna and the connection of the coil, and introducing a machined ceramic piece brazed on the antenna, the cut-off frequency shifts down, and the antenna is able to damp also the resonant modes with low resonant frequencies.

3 MEASUREMENTS

Bench measurements were performed, before the installation, on the new kicker with the antenna to verify the damping efficiency. The wire method was employed to estimate the shunt impedance of the longitudinal and transverse modes trapped in the structure. The old kicker was measured before the installation but only the longitudinal modes were taken into account. When these kickers were removed a complete set of measurements on the longitudinal and transverse plane have been performed.

Figure 4 shows the results of the impedance measurement of the longitudinal trapped modes in the damped and undamped case (comparing the impedance of the old and new kickers). Figure 5 shows the same measurements for the transverse (vertical) modes.

Before the installation the high voltage tests were performed on each kicker. A DC voltage up to 25 KV has been applied in order to test the kicker structure insulation after vacuum treatment.

A test with the power pulser has indicated that the introduction of the antennas does not perturb the shape of the kicker current pulse.

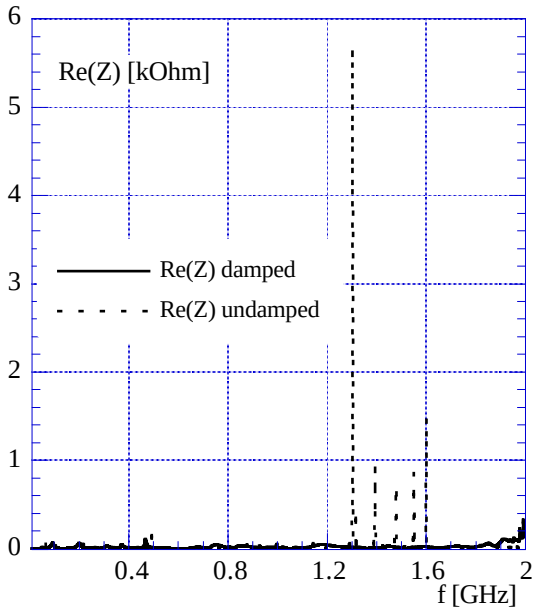

Figure 4: Longitudinal mode impedance with and without damping antenna

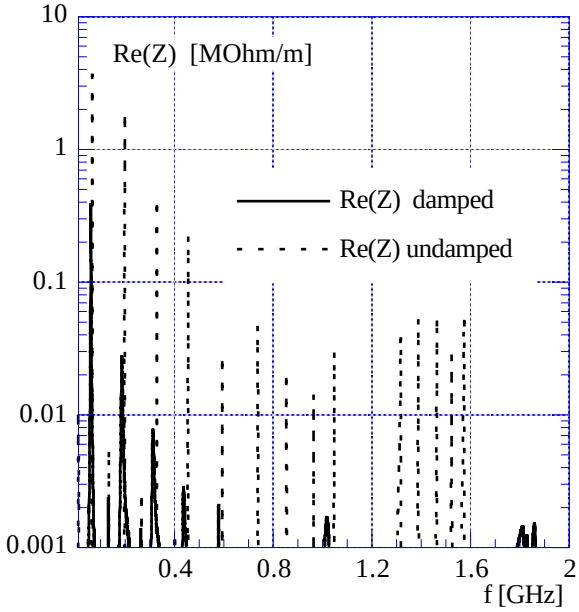

Figure 5: Vertical mode impedance with and without damping antenna

4 CONCLUSION

The bench measurements on the kickers with the damping antennas have shown that the impedances of the dangerous HOM have been reduced to a negligible value. During the machine run some observations of the instability threshold versus the beam displacement in the kicker region have shown the effectiveness of the damping antenna.

AKNOWLEDGMENT

The authors wish to thank S. De Simone for the useful discussions; S. Pella, G. Sensolini and A. Zolla for the technical support.

REFERENCES

[1] D.J. Fox et al., “Programmable DSP-based multi-bunch feedback operational experience from six installations”, BIW, 8-11 May 2000, Cambridge, Massachusetts.

[2] D. Alesini, S. De Simone, A. Gallo, A. Ghigo, F. Marcellini, “DAΦNE Injection Kicker: Electromagnetic Analysis of Trapped Modes and Damping Antenna Design”, International Workshop on Performance Improvement of Electron-Positron Collider Particle Factories (e+e- Factories'99), Tsukuba, Japan, KEK Proc. 99-24, p.146.

[3] S. De Simone, A. Ghigo, “DAΦNE Accumulator Kickers”, EPAC 92 Proceedings, p. 1449, Berlin, March 1992.